

L I C E N C E   T O   M c M A S T E R   U N I V E R S I T Y

This Thesis has been written  
[Thesis, Project Report, etc.]

by Cameron C. Bell for  
[Full Name(s)]

Undergraduate course number 4K6 at McMaster  
University under the supervision/direction of \_\_\_\_\_  
Dr. J.H. Crocket

In the interest of furthering teaching and research, I/we  
hereby grant to McMaster University:

1. The ownership of 3 copy(ies) of this work;
2. A non-exclusive licence to make copies of this work, (or any part thereof) the copyright of which is vested in me/us, for the full term of the copyright, or for so long as may be legally permitted. Such copies shall only be made in response to a written request from the Library or any University or similar institution.

I/we further acknowledge that this work (or a surrogate copy thereof) may be consulted without restriction by any interested person.

James H. Crocket  
Signature of Witness,  
Supervisor

Cam Bell  
Signature of Student

April 24, 1987  
date

ORE PETROGRAPHY,  
CARBONATE ALTERATION AND GEOCHEMISTRY  
OF THE McBEAN MINE,  
LARDER LAKE, ONTARIO.

CAMERON C. BELL

A THESIS SUBMITTED AS PARTIAL FULFILLMENT  
FOR THE HONOURS BACHELOR OF  
SCIENCE DEGREE

FACULTY OF SCIENCE  
McMASTER UNIVERSITY  
HAMILTON, ONTARIO  
APRIL, 1987





CHAPTER 5	GEOCHEMISTRY	51
	5.1 Bulk Composition	51
	5.2 Trace Element Geochemistry	61
	5.3 Rare Earth Element Geochemistry	68
CHAPTER 6	CONCLUSIONS, RECOMMENDATIONS FOR FURTHER RESEARCH AND EXPLORATION IN THE LARDER LAKE AREA	78
	6.1 Conclusions	78
	6.2 Recommendations for Further Research and Exploration in the Larder Lake Area	80
REFERENCES CITED		81
APPENDIX 1		85
APPENDIX 2		88
APPENDIX 3		92

## LIST OF FIGURES

FIGURE	PAGE
1a. Location Map of the Abitibi Greenstone Belt	2
1b. Location Map of the McBean Mine	2
2. Stratigraphic Section of the Larder Lake Area	3
3. McBean Mine Level 1 Ramp	9
4. Bench Number 1 Geology Plan	17
5. Relative Proportions of Carbonate Cation Counts at common energy levels in sample RX67899	42
6. Relative Proportions of Carbonate Cation Counts at common energy levels	43
7. Jensen Cation Plot	57
8. Theoretical Fields of Carbonates on a plot of CO <sub>2</sub> versus CO <sub>2</sub> /CaO molar ratio	60
9a. REE envelope of Archean Syenites	70
9b. REE Pattern for Massive Syenites from Macassa Mine	70
9c. Normalized REE Plot of Massive Syenites from McBean Mine	70
10. Normalized REE Plot of Gneissic Syenites north of the main ore zone.	71
11. Plot of $\Sigma$ HREE versus SiO <sub>2</sub> and CO <sub>2</sub>	74
12. Plot of $\Sigma$ LREE versus SiO <sub>2</sub> and CO <sub>2</sub>	75

## LIST OF TABLES

TABLE	PAGE
1. Major Element Abundances and Normative Minerals	52-53
2. Average Bulk Composition Range of Typical Syenite and Bulk Composition of Unaltered and Altered-Mineralized Felsic Syenite from Macassa Mine	55
3. Trace Element Abundances by INAA	62-63
4. Interelement Correlation Coefficient Matrix	64

## LIST OF PLATES

PLATE	PAGE
1. Ore zone seen in east wall of McBean Pit	12
2. Massive Syenite body in ore zone	12
3. Massive Syenite and Gneissic Syenite at northern boundary of ore zone	13
4. Mylonitized conglomerate near "Larder Lake Break"	14
5. Mylonitized conglomerate near "Larder Lake Break"	15
6. Gold in an intergranular setting between pyrite	34
7. Gold inclusion in pyrite and gold plating on pyrite	34
8. Gold plating on pyrite	35
9. Free gold grains in gangue	35
10. Ilmenite exsolution from magnetite	36
11. Pyrite replacing magnetite	36
12. Gold plating on pyrite and chalcopyrite	37
13. Gold inclusion in pyrite	37
14. Relict ilmenite laths, magnetite and gold found in an inclusion in pyrite	38
15. Ilmenite veinlet beside aggregate of rutile laths	38
16. Backscatter Electron Image of ilmenite veinlet	46
17. Transmitted light, photomicrograph of area in Plate 16	46
18. Backscatter Electron Image of Gneissic Syenite	47

19. Transmitted light, photomicrograph of area in Plate 18	47
20. Backscatter Electron Image of carbonate veinlet	48
21. Transmitted light, photomicrograph of area in Plate 20	48
22. Backscatter Electron Image of carbonate lining a quartz veinlet	49
23. Transmitted light, photomicrograph of area in Plate 22	49
24. Secondary Electron Image of Talc-Chlorite- Schist	50
25. Transmitted light, photomicrograph of area in Plate 24	50

## ACKNOWLEDGEMENTS

This thesis could not have been completed without the co-operation and financial assistance of Inco Limited. In particular I would like to thank: Terry MacGibbon, Joe Church, Wayne Mason and Jon Gill.

I would like to express my appreciation to Dr. J.H. Crocket for his supervision and funding of this thesis.

Many people at McMaster contributed to this thesis. Thanks for technical assistance are extended to O. Mudroch, A. Kabir, J. Whorwood, L. Zwicker and J. Cker. Thanks are also owed to B. McInnes and R. Moritz for their helpful comments.

Special thanks go to my family and Marsha Clapham for their patience and support.



## ABSTRACT

The McBean Mine is a small gold producer located along the Larder Lake Break. Ore from the open pit consists of massive and gneissic syenite. The highest gold grades come from highly carbonitized syenitic rocks with abundant fine grained, euhedral pyrite. Petrographic observation shows gold to be found as inclusions in pyrite, platings on pyrite and as free grains in the gangue. XRD analyses show the major carbonate type to be dolomite. In addition to dolomite, minor amounts of calcite are found in auriferous syenitic rocks. SEM microscopy shows carbonate composition to vary with rock types and grain location. Geochemical studies show a high intensity of carbonate alteration and the association of gold with tungsten and uranium. Auriferous syenites were determined to have elevated HREE element abundances compared with unaltered syenite. The mine is therefore characterized by extensive hydrothermal carbonate alteration related to the Larder Lake Break.

## CHAPTER 1 GENERAL GEOLOGY

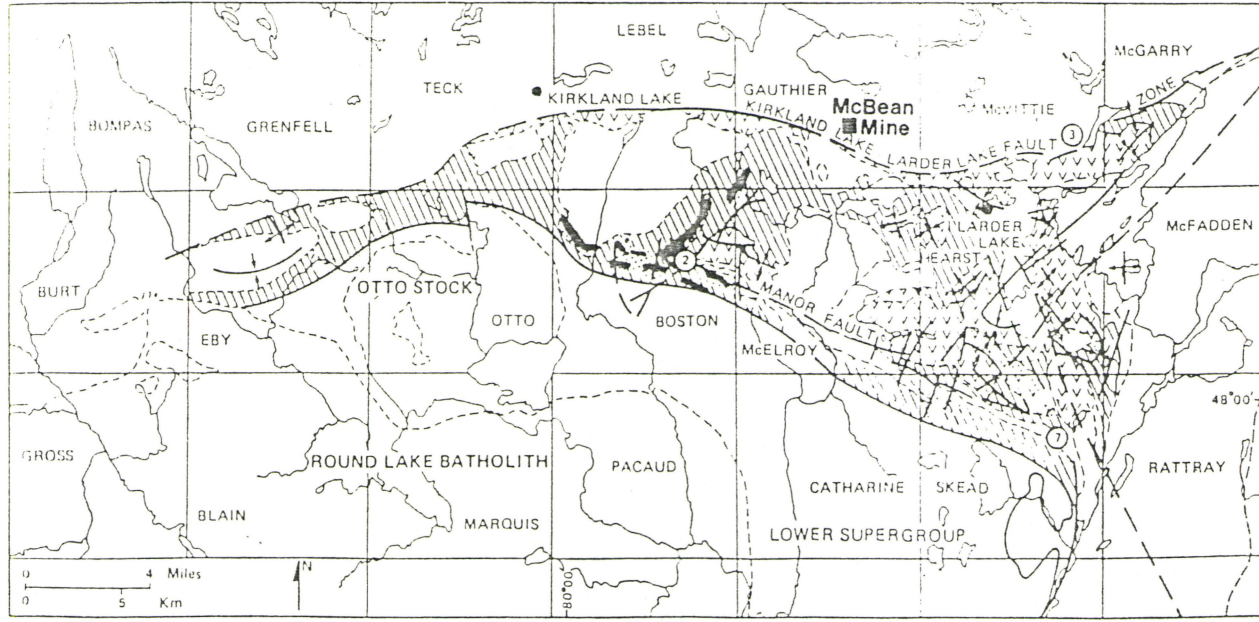
### 1.1 Regional Geology

The McBean Mine is located in the Abitibi Greenstone belt 7km northwest of the town of Larder Lake. The belt straddles the Ontario-Quebec border and is approximately 800 km long and 240 km wide (Fig. 1a). In the southern Kirkland Lake area, Archean rocks are unconformably overlain by Proterozoic sediments of the Cobalt Group. The belt is cut by swarms of Matachewan dikes and by Keweenawan diabase dikes. In the Kirkland Lake area volcanic rocks of the Abitibi Belt are preserved in a synclinorium between the Abitibi Batholith and the Round Lake Batholith (Jenson and Langford, 1985). The axis of the synclinorium occurs halfway between the two batholiths and plunges to the east. The northern limb of the synclinorium is cut by the Kirkland Lake-Larder Lake fault zone. The Archean rocks in the belt have been metamorphosed to the sub-green schist facies (Jolly, 1978). In the Kirkland Lake area the stratigraphy consists of supergroups representing cycles of ultramafic to felsic volcanism. In the Kirkland Lake area two complete volcanic sequences are present. A stratigraphic section showing the groups present in the Larder Lake area is shown in Fig. 2.

The open pit at the McBean Mine is located directly adjacent to the Larder Lake Break (see Fig.1b for location). The Larder Lake Break is part of the Kirkland Lake-Larder



Figure 1a  
Location Map of the Abitibi Greenstone Belt



**LEGEND**

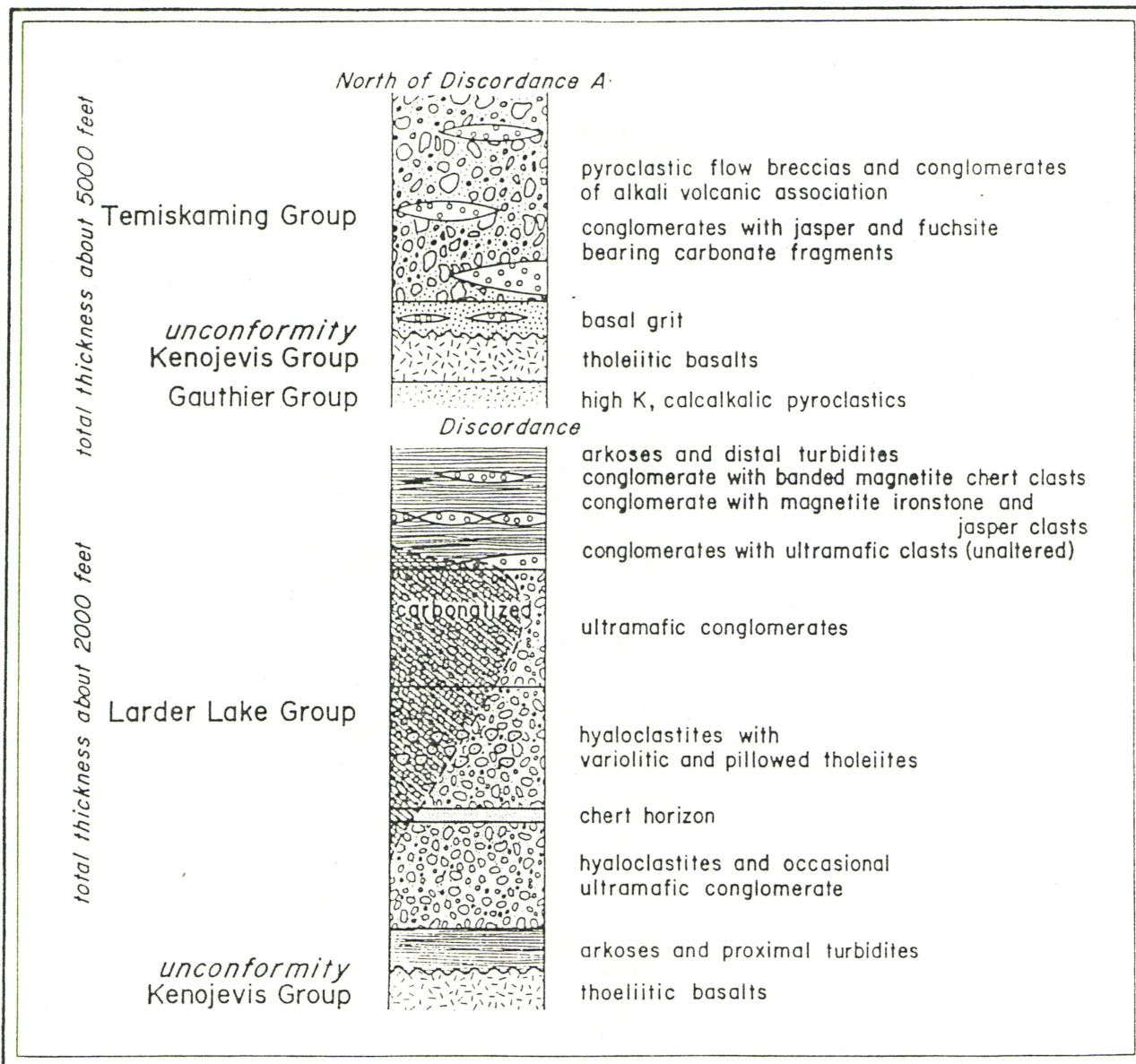
- Fault
- Syncline
- Anticline
- Geological Boundary
- Location

**LARDER LAKE GROUP**

- Iron Formation
- Turbiditic sedimentary rocks
- Calc - alkalic felsic tuffs & tuff breccia
- Komatiitic & tholeiitic lavas

Figure 1b  
Location Map of the McBean Mine

Figure 2 Stratigraphic Section of the Larder Lake Area



-after Downes, 1981



Lake fault zone. The exact nature of the Larder Lake Break is a matter of some controversy. It is classically referred to as a linear feature of limited lateral extent that shows strong foliation and carbonatization in mafic rocks (Thomson, 1943). Ridler (1970) put forward the idea that the Larder Lake Break does in fact not exist, but, is a zone of strong foliation located within the easily deformed carbonate rocks of the Timiskaming. Thomson (1950) believed the break was a major fault which triggered hydrothermal carbonate alteration. Several authors (Thomson 1943, Hewitt 1963, Ridler 1970) believe that the sediments on either side of the break are Timiskaming in age. Jensen and Langford (1985) believe the sediments south of the break to be of the Larder Lake Group. They propose that the Timiskaming Group is faulted against the Larder Lake Group along its southern boundary. They also put forward the theory that the Timiskaming Group was formed and preserved in a narrow graben with a scarp on its southern side.

Mapping by Downes (1981) shows that significant structural discordances are found on either side of the Larder Lake Break including changes in fold-axes plunge and lineation plunge. At the Kerr Addison Mine ore bodies straddling the Kerr Fault change plunge from approximately 65 degrees east on the north side to 50 degrees southwest on the south side (Downes, 1981). In Hearst Township a northwest trending foliation ends abruptly at the break (Toogood and

Hodgson, 1985). Thus, the Larder Lake Break can be described as a major structural discontinuity.

The Timiskaming Group is found to the north of the Larder Lake Break for a distance of 60km along the break with a width of 4km north of the break. These rocks consists of K-rich alkalic and calc-alkalic rocks which are interlayered with fluvial sediments. Dikes and stocks of syenite, monzonite and quartz monzonite cut the Timiskaming Group (Jensen and Langford, 1985). The Upper Canada Mine is located just to the north of the McBean open pit in trachytic metavolcanics of the Timiskaming Group.

In the vicinity of the McBean Mine the rocks south of the Larder Lake Break are known as the Larder Lake Group. The Larder Lake Group is a komatiitic succession found south of the break which widens towards the Ontario-Quebec border. The Larder Lake Group consists of calc-alkalic rhyolite tuff-breccias and tuffs, clastic sediments, iron formation, limestone, dolomite, and komatiitic and tholeiitic lavas (Jensen and Langford, 1985). The sediments of the Larder Lake Group are considered to be turbidites. The members of the Larder Lake Group have been isoclinally folded and Jensen and Langford (1985) believe that the group was formed on a broad shelf between an elevated area to the south and a marine basin to the north.

## 1.2 Economic Geology

In 1985 5 gold mines were in production in the Kirkland Lake area. Four of these mines; the Kerr Addison Mine at the northeastern tip of Larder Lake, the McBean Mine near Dobie, and the Macassa and Lakeshore mines in Kirkland Lake are located along the Kirkland Lake-Larder Lake Break. Between Kenogami Lake and the Kerr Addison Mine there are 32 known gold deposits (Tihor, 1978). These are almost all situated along the Kirkland Lake-Larder Lake fault zone. In Lebel and Teck Townships gold generally occurs in quartz veins in syenites and sediments and along, or proximal to, structural breaks. Farther east in the Larder Lake area gold often occurs in quartz stockworks in carbonate zones. These carbonate zones include many rock types: dacites, syenites, tuffs and talc-chlorite schists (Goodwin, 1965).

The ore at Kerr Addison occurs in two types. Gold occurs in a "green carbonate" host which is described as a fuchsite-bearing dolomitized ultramafic volcanic rock. Associated with this metasomatic alteration are quartz veins containing free gold (Downes, 1981). The other type of ore at Kerr Addison is flow ore. This ore is composed of several lithological types most of which are altered intermediate to mafic volcanics and which are, without exception pyritic. It is the pyrite in these ores which hosts the gold (Downes, 1981). By the end of 1984 the Kerr Addison Mine had produced 563, 958 oz. of gold (Lovell, 1986).



At the Lakeshore Mine in Kirkland Lake the ore zones are mainly hosted by syenite porphyry. The ore is composed of quartz vein systems with calcite, dolomite and chlorite. The gold at the Lakeshore Mine is carried by tellurides and as native gold (McInnes, 1985). By the end of 1984 the Lakeshore Mine had produced 1,955,132 oz. of gold (Lovell, 1986). The syenites at the Lakeshore Mine are good host rocks as they undergo brittle fracture at high stress. This forms a conduit for gold bearing hydrothermal solutions (Colvine et al, 1984).

The ores at the Macassa Mine are deposited in volcanic and sedimentary rocks intruded by a syenite stock (Kerrich and Watson, 1984). At the Macassa Mine there are three types of gold ore. Break ore consists of native gold in chloritic fault gouge and in small quartz lenses found along a thrust fault system. Auriferous quartz veins, termed vein ore, are found in the wall rock along the fault system. These veins contain quartz, wall rock fragments, some dolomite and calcite, disseminated pyrite, precious metal and base metal tellurides, and fine grained native gold. Molybdenite and occasionally graphite, coat fractures in the quartz. Breccia ore consists of intensely fractured, bleached, silicified and pyritized rock. This ore contains lenses of quartz native gold and tellurides (Kerrich and Watson, 1984). By the end of 1984 the Macassa Mine had produced 2, 583, 157 oz. of gold (Lovell, 1986).

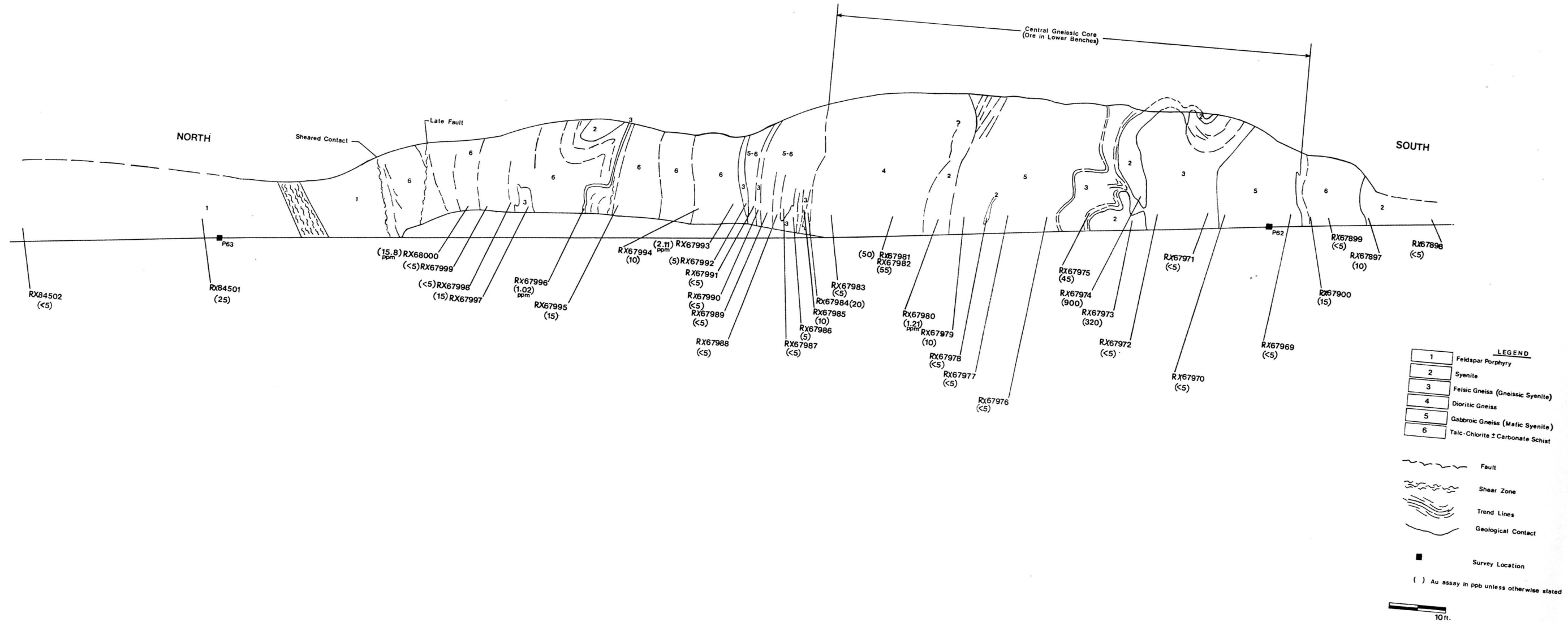
At the Upper Canada Mine gold is hosted by trachytic flows and sediments, and is often found in red chert bands in the trachytic flows, adjacent to parallel shear zones. Syenite dikes have intruded and altered the volcanic units. The alteration accompanying the shear zones is characterized by carbonate, sericite and chlorite (Stewart, 1986). Before it was shut down the Upper Canada Mine produced 1,398,291 oz. of gold.

### 1.3 McBean Mine Geology

The McBean Mine open pit began operation in May of 1984. Mining continued until the spring of 1986. During the operation of the pit seven benches were blasted out and mined. The ore consisted of northeast trending, near vertical syenitic blocks. To the south of the ore zone is a non-auriferous syenite and a talc-chlorite-carbonate schist which extends southward until it contacts a gabbro unit. The ore zone contains alternating units of mafic syenite, syenite, and gneissic syenite (felsic "gneiss"). A dioritic gneiss unit is also part of the ore zone (Pattison, unpublished map). The zone representing ore in the lower benches and rocks to the north and south along the level 1 ramp can be seen in Fig.3. For the sake of consistency the zone designated as ore in the lower benches along the level 1 ramp by Pattison (unpublished map) will be termed the ore zone for the remainder of this study. The syenites along the

# McBean Mine Level 1 Ramp

Sample Locations, Au Assays, Geology



Map Adapted After Pattison, 1985

level 1 ramp ore zone do not make ore grade as will be discussed later. The east wall of the ore zone for the pit as a whole can be seen in Plate 1. The syenitic units along the level 1 ramp ore zone and the syenitic units to the north of the ore zone are shown in Plates 2 and 3. In the zone immediately to the north of the ore zone the rocks have been intensely folded and boudinaged. This zone is bordered to the north by talc-chlorite schist which contains numerous blocks and bands of syenite and gneissic syenite (some of which are highly auriferous). This talc-chlorite schist envelops the ore body. A block of feldspar porphyry is contained within this unit to the north of the zone. To its north the talc-chlorite schist contacts a mylonitized conglomerate. This contact is thought to be part of the Larder Lake Break (McBean Mine Geology Plans). At this contact a discrete fault with the usual accompanying fault gouge was not observed. In the McBean Pit the Larder Lake Break takes the form of a zone of deformation. Shear zones, small faults and locally intense foliation are present in the talc-chlorite schist and feldspar porphyry to the north of the ore zone. The sediment to the north of the "Break" is probably Timiskaming group. Conglomerate in the Timiskaming is thought to be fluvial in origin (Jensen and Langford, 1985). This conglomerate is highly mylonitized and contains smeared out clasts of chert and volcanic rock. This unit is shown in Plates 4 and 5. This rock was examined microscopically and was found to have clasts with axial

ratios (a:c axes) of 20:1 in some cases (P.M. Clifford, personal communication).

By the end of 1984 9,002 oz. of gold had been recovered from the open pit at McBean Mine. Low grade ore recovered from the mine was 0.05+ oz./ton while higher grade ore was 0.1+ oz./ton. The average grade of ore recovered from the mine was 0.087 oz./ton. The seventh bench, the last level mined produced 3990.5 oz. of gold at an average grade of 0.111 oz./ton with the highest grade ore running 0.15 oz./ton. Cleanup of the ore was completed in the summer of 1986. In total the mine produced 46,153 oz. of gold. Due to new, highly efficient cyanide recovery techniques the mine was able to produce at relatively low grades. Mine personnel believe that the gold was carried by syenitic rocks containing fine grained pyrite. The colour of the syenite was believed to give some indication of the grade and syenite of a purple colour was thought to carry the highest gold concentration.

Plate 1: Ore zone seen in east wall of McBean Pit.  
Syenitic ore is stained reddish brown due to  
oxidation of pyrite.

Plate 2: Massive Syenite (sy) body in ore zone.







Plate 3: Massive syenite (ms) and gneissic syenite (gs) at northern boundary of ore zone.

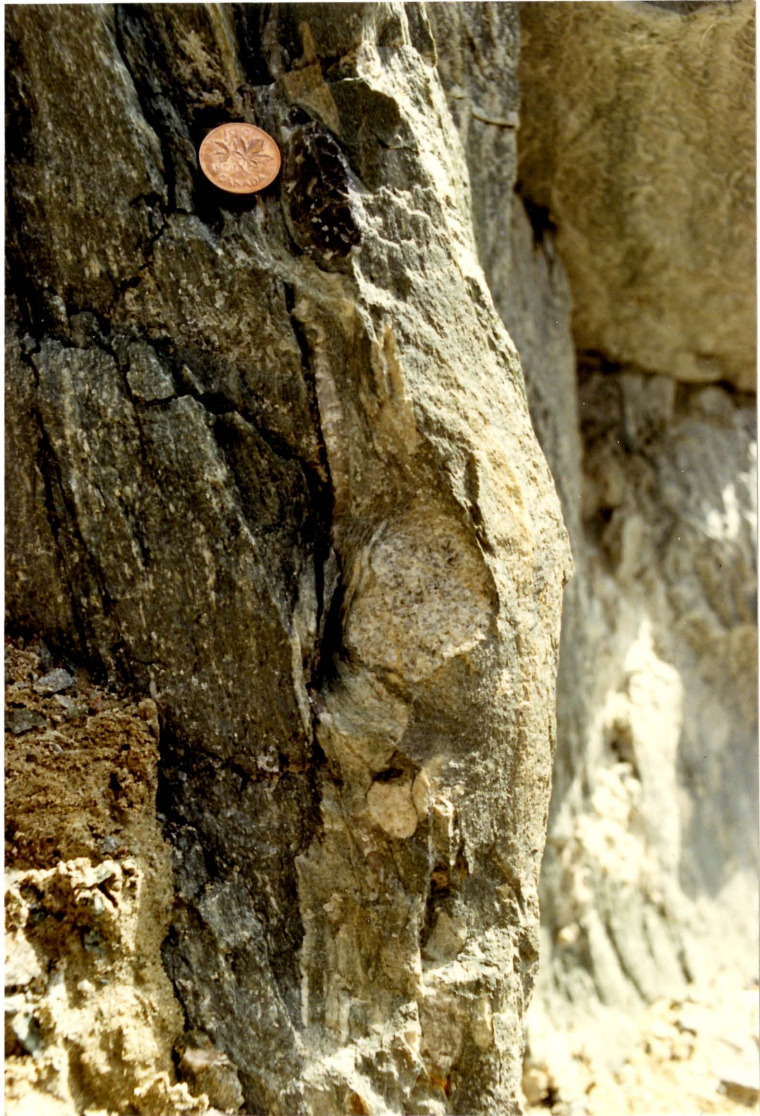


Plate 4: Mylonitized conglomerate near "Larder Lake Break".  
Light coloured streaks are smeared out clasts.



Plate 5: Mylonitized conglomerate near "Larder Lake Break".  
Note the polymictic nature of the conglomerate.





## CHAPTER 2 METHODOLOGY

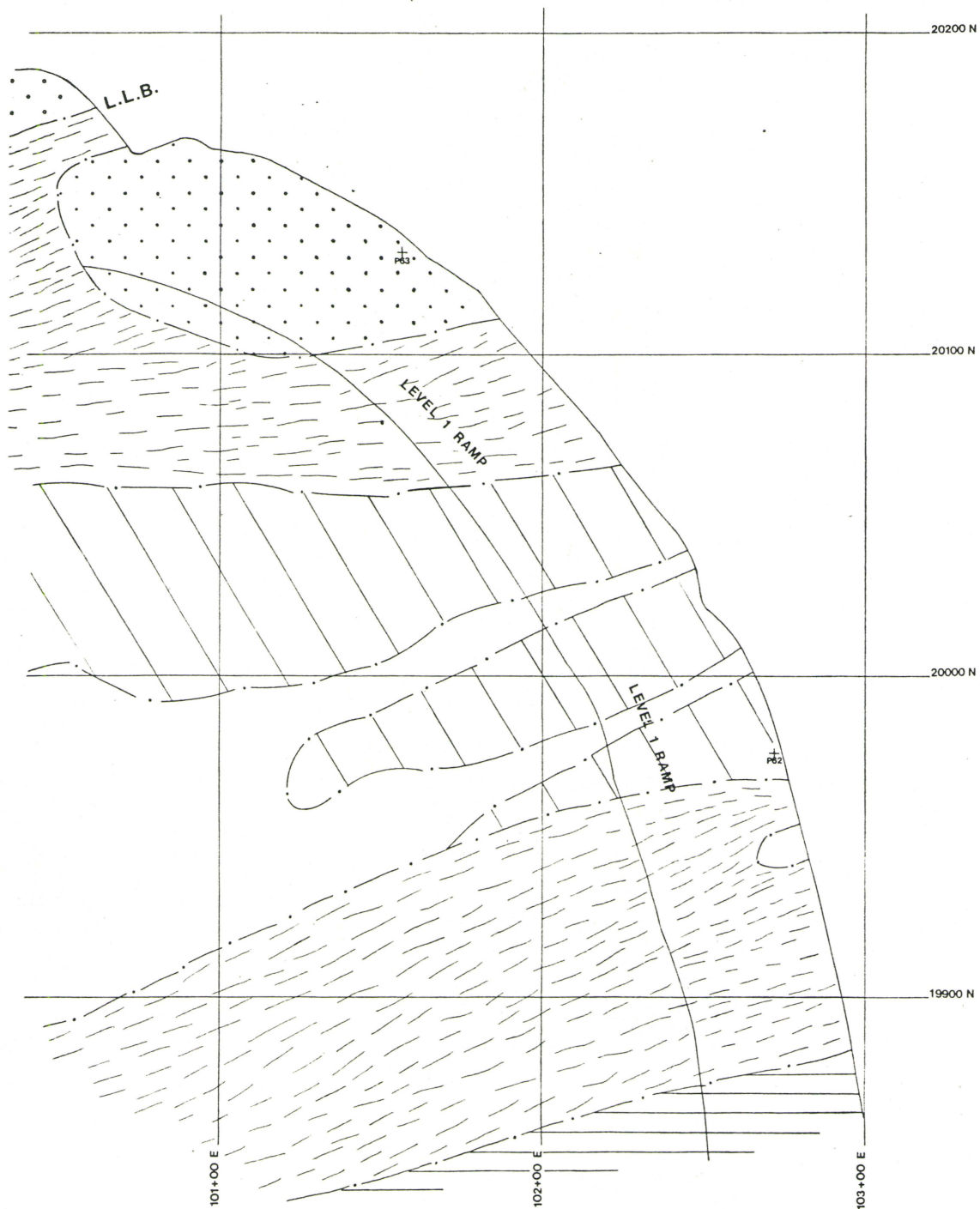
### 2.1 Sampling Methods and Gold Assay Results

Samples were collected on August 26 and 27 during the summer of 1986. The sampling was carried out along the level 1 ramp as it had the safest ground and the best exposure of the ore zone. At least one sample was taken from each unit across the level 1 ramp as it had the safest ground and the best exposure of the ore zone. The section sampled was from 30 ft. south of survey point 62 to 35 ft. north of survey point 63. Sample locations can be seen in Figure 3. The section of the open pit sampled is shown in plan view in Figure 4.



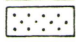



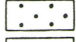
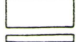

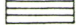
Gold was analysed by fire assay courtesy of Inco Ltd. The assay results are plotted in Figure 2. The highest gold values came from narrow bands of gneissic syenite to the north of the ore zone. The highest assay in these rocks was 15.8 ppm. In the ore zone massive syenites carried the greatest concentrations of gold (to 1.21 ppm). Background gold values were <5 to 10 ppb. Condensed sample descriptions and gold assays can be found in Appendix 1.



Figure 4 Bench No. 1 Geology Plan



LEGEND

- |                                                                                     |                      |                                                                                     |                    |
|-------------------------------------------------------------------------------------|----------------------|-------------------------------------------------------------------------------------|--------------------|
|  | Talc-Chlorite Schist |  | Geological Contact |
|  | Feldspar Porphyry    |  | Pit Wall           |
|  | Mafic Syenite        |  | Survey Location    |
|  | Conglomerate         |                                                                                     |                    |
|  | Syenite              |  | 20ft.              |
|  | Gabbro               |                                                                                     |                    |

## 2.2 Analytical Methods

### 2.2.1 Fire Assay

40 samples from the level 1 ramp were analysed for Au at Inco Ltd.'s Copper Cliff Exploration Geochemical Lab. The samples were crushed to finer than -200 mesh and then fire assayed. The detection limit for this assay is 5 ppb.

### 2.2.2 X-Ray Diffraction

X-Ray Diffraction (XRD) was performed on four samples from the level 1 ramp. With this method of analysis calcite, siderite, magnesite and the dolomite-ankerite solid solution series can be relatively accurately identified. Several other minerals in the samples were also identified including quartz, albite, chlorite, talc, pyrite and microcline. A drawback of XRD is that it is difficult to distinguish between dolomite, ferroan dolomite and ankerite. The primary peak of dolomite occurs at 30.985  $2\theta$  while ankerite's primary peak is 30.952  $2\theta$ . Another drawback to this method is that it does not provide quantitative results.

The material used in the XRD analysis was pulp from rock samples crushed to finer than -200 mesh size. This material was slurried onto a glass slide with acetone and permitted to dry. The samples were then scanned from 5 to 55 degrees two theta at a rate of one degree per minute. For this analysis Copper K radiation produced at 30kV and 16mA was used.

Primary and major secondary  $2\theta$  peaks were identified and their  $d$  spacings were calculated using Bragg's equation  $\lambda = 2d \sin\theta$ . The diagnostic  $d$  spacings and peak intensities for mineral identification were taken from the Joint Commission of Powder Diffraction Standard Files.

### 2.2.3 Major Element Analysis

X-Ray Fluorescence (XRF) was used to determine the major element abundances of 10 samples taken along level 1 ramp of the open pit. Powder pellets of samples ground to finer than -200 mesh were analysed on a model PW1450 Philips automatic sequential spectrometer. Precision of the major element analysis should be similar to the following levels:  $\text{SiO}_2$  2%,  $\text{Al}_2\text{O}_3$  3%,  $\text{Fe}_2\text{O}_3$  and  $\text{CaO}$  4%,  $\text{MgO}$  and  $\text{Na}_2\text{O}$  5-10%. Absolute deviations of 0.01-0.02% are usual for  $\text{MnO}$ ,  $\text{TiO}_2$ , and  $\text{P}_2\text{O}_5$  (O.Mudroch, personal communication). The accuracy of the XRF analysis in terms of relative error with 95% certainty are as follows:  $\text{SiO}_2$  2%,  $\text{Al}_2\text{O}_3$  3%,  $\text{Fe}_2\text{O}_3$  and  $\text{CaO}$  4%,  $\text{MgO}$  and  $\text{Na}_2\text{O}$  5-10%. The absolute error of the results of  $\text{TiO}_2$ ,  $\text{MnO}$  and  $\text{P}_2\text{O}_5$  will be equal to 0.01 to 0.04% (O.Mudroch, personal communication).

### 2.2.4 Carbon Dioxide

Total carbon was determined using a Leco model 761-100 automatic carbon determinator. This analysis is based on gas

thermal conductivity. The total carbon content is then recalculated as CO<sub>2</sub>. The precision of this analysis at CO<sub>2</sub> abundances below 1wt.% ranges between 10 and 40%. At CO<sub>2</sub> abundances between 1 and 30wt.% is better than 4%. The accuracy of this analysis is better than 5% at the 1 to 30wt.% CO<sub>2</sub> level (Fyon et al, 1983). The H<sub>2</sub>O wt.% can be calculated by subtracting the CO<sub>2</sub> content from the Loss on Ignition (LOI) value. Samples with no apparent H<sub>2</sub>O present probably have erroneously high CO<sub>2</sub> values. This is caused by the oxidation of some of the sulphide and its partial inclusion in the CO<sub>2</sub> value. The CO<sub>2</sub> weight percents were corrected by determining sulphur values.

#### 2.2.5 Loss on Ignition

Weighed samples crushed to finer than -200 mesh were ignited at 1000 C for 30 minutes and reweighed to determine the LOI. At the LOI values encountered the accuracy and precision is better than 2% (Fyon et al, 1983). The LOI is a measure of the decrease in weight which occurs when H<sub>2</sub>O, CO<sub>2</sub> and possibly SO<sub>2</sub> are vaporized at high temperatures. These oxides represent the volatile component of the various samples.

### 2.2.6 Trace Element Analysis

The concentration of 26 elements was determined for a suite of 10 samples. These concentrations were found by Instrumental Neutron Activation Analysis (INAA). INAA was performed on approximately 6 grams of sample crushed to finer than -200 mesh. These samples were sealed in poly vials and irradiated for 10 minutes in the thermal neutron flux of the McMaster University pool type reactor. The concentrations of the 26 elements were then counted on a coaxial intrinsic germanium detector (APTEC Engineering Company, Toronto). The detection limit for each element is as follows:

<u>Element</u>	<u>Detection Limit</u>	<u>Element</u>	<u>Detection Limit</u>
Ag	5.0 ppm	Sc	0.1 ppm
As	2.0 ppm	Se	5.0 ppm
Au	5.0 ppm	Ta	1.0 ppm
Ba	100.0 ppm	Th	0.5 ppm
Ca	1.0 %	U	0.5 ppm
Co	5.0 ppm	W	4.0 ppm
Cr	10.0 ppm	Zn	50.0 ppm
Fe	0.02 %	La	1.0 ppm
Hf	1.0 ppm	Ce	3.0 ppm
Mo	5.0 ppm	Sm	0.1 ppm
Na	0.05 %	Eu	0.2 ppm
Ni	200.0 ppm	Yb	0.2 ppm
Sb	0.2 ppm	Lu	0.05 ppm

-analyses performed by Nuclear Activation Services

### 2.2.7 Scanning Electron Microscopy

The Scanning Electron Microscope (SEM) allows for the semi-quantitative analysis of individual grains in a sample. Four samples from the level 1 ramp were examined. Thin



sections from these samples were examined on a transmitted light microscope. Specific areas of approximately 0.7cm<sup>2</sup> were selected on the basis of the presence of carbonate in various forms (veinlets, vein linings, main portion of sample) and non-identifiable minerals. The thin sections had their cover slips removed and were cleaned by acetone and air pressure hose. The portion of the slide to be examined by the SEM was then cut from the rest of the slide using a minierature ban saw. These thin section portions were then coated with carbon and sealed along the rock-glass boundary.

The SEM unit used was a Philips model 515 scanning electron microscope. The samples are placed on a stage in a vacuum chamber during analysis. A backscatter electron image or a secondary electron image can be used for diagnostic purposes. The back scatter electron image shows the composition of the grains based on atomic mass. Heavier atomic mass grains will show up light gray or white while lighter atomic mass compounds will be a dark gray. The secondary electron image shows only surface relief of a grain. The SEM can analyse a point on the surface or an area of a grain. This analysis accounts for all elements present accept for carbon and oxygen. When bombarded with an electron beam each element emits X-rays at a specific energy. The SEM gives the counts at a certain energy for the elements present.

The main purpose in using the SEM was to study the distribution of the various cations present in the

carbonates. The true ratios of the cations cannot be determined by this microscope, so it is not possible to determine for example, if the carbonate in a particular sample is an ankerite (Fe:Mg ratio of  $>1:4$ ). Thus, the ratio of the counts for the various cations in carbonates does not represent their absolute proportions in the cation position of the carbonate crystal structure. The backscatter electron output of this SEM can determine changes in the relative proportions of the cations from one carbonate grain to another in the sample. It can therefore be determined if one grain is depleted in the relative proportion of a certain cation compared with another grain.

## CHAPTER 3 PETROGRAPHY

### 3.1 Transmitted Light Petrography

#### 3.1.1 Talc-chlorite Schist

This rock is highly schistose and contains elongated augen-like aggregates of carbonate up to 3mm in length. These carbonate aggregates are in a matrix of talc, chlorite and opaques which are in parallel orientation. A grain of carbonate set in this matrix can be seen in Plate 25 .

#### 3.1.2 Massive Syenite

South of the ore zone the syenite contains relatively unaltered plagioclase grains with minor orthoclase. The plagioclase grains are of albite composition and are relatively large (to 1.3mm). These grains are set in a matrix of fine grained feldspar and anhedral carbonate. Carbonate may constitute up to 10% of the thin section. In the ore zone the massive syenites are finer grained with plagioclase grains up to 0.8mm. The plagioclases display deformation textures such as disrupted and bent twinning. Most plagioclase grains contain inclusions of sericite. Veinlets of carbonate up to 0.8mm in width are present along with carbonate lined quartz veins with widths >1cm (see Plates 21 and 23). The amount of non-vein carbonate in the ore zone syenite is approximately the same as the syenite to the south.

### 3.1.3 Mafic Syenite

These rocks contain relatively little unaltered feldspar. Carbonate and chlorite are the dominant mineral components. Biotite, quartz and altered plagioclase are also present. Some samples contain biotite as a major component (to 20%) and altered pyroxene grains.

### 3.1.4 Dioritic Gneiss

These weakly banded rocks do not show gneissosity at the thin section scale. Carbonate is pervasive in dioritic gneiss with the finer grained samples containing greater carbonate abundances. Coarser grained varieties contain heavily sericitized feldspar grains up to 1.5mm in length. Stringers of parallel oriented chlorite grains are pervasive in samples of this rock type. Tabular grains of biotite (to 1.5mm) with bent cleavage traces are common.

### 3.1.5 Gneissic Syenite

In the ore zone gneissic syenites contain abundant carbonate with minor sericitized feldspar. A sample of this rock type can be seen in thin section in Plate 19. Subhedral pyrite grains to 0.8mm and large bent biotite grains >1mm in length are locally abundant. Aggregates of subhedral chlorite grains are common. North of the ore zone biotite is rare and the pyrite grains are more euhedral. The pyrite grains commonly form lineations along stringers of chlorite. This rock type is locally banded with carbonate rich and carbonate poor bands. Very fine grained quartz and feldspar

(to 0.1mm) are dispersed throughout. Carbonate veinlets form along fractures which occasionally crosscut sulphide grains.

### 3.2 Ore Petrography

The ore petrography of the McBean Mine was found to be similar to that of the Upper Canada Mine. Thomson (1943) conducted microscopic examinations of ore from the Upper Canada Mine. He found pyrite to be the principle sulphide with lesser amounts of chalcopyrite, galena, specularite and molybdenite. The gangue was found to be quartz-carbonate. Gold occurred in a finely divided condition in both the pyrite and gangue. The gold associated with pyrite was mainly concentrated along sinuous fractures in pyrite grains. The ore from Upper Canada was treated by straight cyanidation.

#### 3.2.1 Pyrite

At the McBean Mine pyrite was also found to be the most abundant ore mineral. This sulphide is common in samples from the level 1 ramp. Syenite south of the ore contained large euhedral grains of pyrite up to 0.5mm and finer subhedral grains to 0.5mm. In massive syenite from the ore zone pyrite occurs in two forms: as aggregates of subhedral grains to 3mm and in small euhedral grains to 0.5mm. The aggregates of pyrite probably represent large grains which have been fractured and have undergone recrystallization and replacement by gangue. Pyrite was found to be embayed by



rutile, chlorite, white mica, quartz and fine grained feldspar.

In gneissic syenite bands from north of the ore zone pyrite may constitute as much as 20% of the section. These pyrite grains are euhedral to subhedral and up to 1mm in diameter. They form lineations with chlorite and white mica. These lineations occur in the plane of gneissosity and are often found at the edge of carbonate-rich bands where pyrite may form as a replacement of magnetite. This texture can be seen in Plate 11. The most common deformation texture in pyrite in gneissic syenites north of the ore zone is brittle fracturing. Fractured pyrite grains are occasionally crosscut by carbonate veinlets. Chalcopyrite and gold have filled pyrite fractures in places. In the gneissic syenites pyrite is commonly replaced along grain boundaries by ilmenite and rutile. Anhedral inclusions as large as 50u of pyrrhotite and chalcopyrite are occasionally found in pyrite.

### 3.2.2 Magnetite

Magnetite in the rocks at McBean is probably of magmatic origin because grains not replaced by pyrite are very euhedral. The magnetite present at McBean is titaniferous as grains often contain exsolution lamellae of ilmenite. Euhedral magnetite with exsolution of ilmenite can be observed in Plate 10. When magnetite is replaced by pyrite and gangue ilmenite lamellae often remain unreplaced (see Plate 14). Some magnetite grains contain anhedral inclusions of chalcopyrite. Magnetite is most common in gneissic

syenites north of the ore zone, but, is rare in syenites in the ore zone.

### 3.2.3 Gold

At McBean native gold was found only in gneissic syenites north of the ore zone. Gold in the ore zone may be carried partly in submicroscopic grains in pyrite. The absence of microscopic gold in the ore zone is probably reflected in the low assay values in syenites. Most gold at McBean was likely carried as free gold grains of microscopic size. This is suggested by the fact that a 94.4% recovery rate was obtained from this relatively low grade ore.

The polished thin sections which contained native gold came from the two samples with the highest gold values. These samples were from gneissic syenite north of the ore zone (RX68000 and RX67996). Gold occurs as free grains in gangue, rimming pyrite, as inclusions in pyrite and along fractures in pyrite.

In sample RX68000 14 gold grains were observed. Eight of these grains were found as free grains in gangue. Of these eight grains, seven were found in quartz-carbonate gangue while one occurred in chlorite. One gold grain was found in an intergranular setting between pyrite grains, two grains were found rimming pyrite and one grain rimmed chalcopyrite. The other two grains were found as inclusions in pyrite. Plate 13 shows a gold inclusion in pyrite. Gold is shown rimming pyrite and chalcopyrite in Plate 12. A gold grain can be seen in an intergranular setting between pyrite

grains in Plate 6. Free gold grains in quartz-carbonate gangue are shown in Plate 9.

Three gold grains were found in the polished thin section of sample RX67996. One grain was observed rimming pyrite while two grains were found as inclusions in pyrite. An inclusion of gold in pyrite and gold rimming pyrite are shown in Plate 7.

#### 3.2.4 Ilmenite

Ilmenite occurs as veinlets and free grains in the ore zone. An ilmenite veinlet can be observed in Plate 15. In some ilmenite grains twinning lamellae were observed under crossed polars. In the gneissic syenite north of the ore zone ilmenite occurs as exsolution lamellae in magnetite, in laths up to  $70\mu$ , in larger subhedral grains and as a replacement of pyrite around pyrite grain edges. Exsolution of ilmenite from magnetite can be observed in Plate 10. Ilmenite exsolution lamellae can be found in pyrite and gangue as shown in Plate 14. This plate shows pyrite replacing magnetite containing exsolution lamellae. The lamellae of ilmenite were not replaced after pyrite replaced magnetite or after gangue replacement of pyrite.

#### 3.2.5 Rutile

Rutile is present in all polished thin sections. It is found as wispy, anhedral grains to  $100\mu$ . In gneissic syenites north of the ore zone rutile grains form lineations parallel to gneissosity. Rutile is occasionally found replacing pyrite grains along grain boundaries.

### 3.2.6 Chalcopyrite

Chalcopyrite was only observed in samples RX68000 and RX67996 from gneissic syenites north of the ore zone, and is found only in trace abundances. The mineral occurs as small (to 200 $\mu$ ) subhedral grains in gangue, along fractures in pyrite, as anhedral inclusions in magnetite and as rims along pyrite grains. Chalcopyrite is shown in these forms in Plates 11, 13 and 12. Gold was found to rim chalcopyrite as well as pyrite. An example of this can be seen in Plate 12.

### 3.2.7 Pyrrhotite

This mineral is found only in trace amounts as tiny (<50 $\mu$ ) anhedral inclusions in pyrite from gneissic syenite samples north of the ore zone.

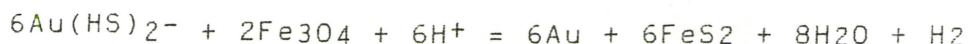
### 3.2.8 Paragenesis

The auriferous rocks of the ore zone have distinctive differences in ore mineralogy and texture compared with gneissic syenites north of the ore zone. Pyrite is found in greater abundances and is less euhedral in the gneissic syenites. Pyrite grains form lineations due to the banding present in the gneissic syenites. This lineation of pyrite grains is not seen in the ore zone. Magnetite and chalcopyrite are by and large absent in the ore zone. Gneissic syenites north of the ore zone have been more highly carbonitized than ore zone massive syenite. These petrographic and compositional differences probably arise from variations in the degree of alteration, magma composition, hydrothermal fluid composition and unit



thickness. The gold bearing gneissic syenites are closer to the zone of deformation associated with the Larder Lake Break and they are found as bands and dikes of much smaller thickness than the syenites in the ore zone. This smaller thickness allows the gneissic syenites to more easily exchange elements with the wall rocks.

At McBean magnetite was first to crystallize and was probably of magmatic origin. Subsequently exsolution of ilmenite from magnetite occurred and replacement of magnetite by pyrite followed. This replacement probably occurred with the initiation of hydrothermal alteration. Solutions involved in hydrothermal alteration were CO<sub>2</sub> rich as evidenced by the pervasive carbonate mineralization. The gold may have been carried in solutions involved with the hydrothermal alteration. Gold may have been transported as a carbonate (AuCO<sub>3</sub><sup>-</sup> or AuCO<sub>3</sub><sup>+</sup>) or a bisulphide [Au(HS)<sub>2</sub><sup>-</sup>] complex. If the gold was carried by bisulphide the following reaction could precipitate gold and cause pyrite to form in the presence of magnetite.



-after Philips et al, 1984

This reaction would consume H<sup>+</sup> ions and raise the pH of the solution. Carbonate is unlikely to precipitate from acidic solutions. A pH change towards a more alkaline solution may account for the intensity of carbonitization found at McBean. If this type of reaction occurred it could explain the lower



gold values in syenites from the ore zone compared with gneissic syenite north of the ore zone. Gold values in the ore zone may be lower as no magnetite was present to trigger the precipitation of gold.

The timing of alteration and the composition of the fluids involved is doubtlessly complex. The presence of repetitions of gold rimming pyrite, which in turn is rimmed by chalcopyrite, can be seen in Plate 12. This indicates that gold precipitation occurred in at least two stages. Regional greenschist facies metamorphism also effected the rocks. The formation of chlorite, biotite, muscovite and rutile at McBean may be related to this metamorphism. The proximity of the mine to the Larder Lake Break and the deformation associated with it have also affected the ore petrography. The Break most likely acted a conduit for fluids involved with hydrothermal alteration. Deformation associated with the break contributed to the fracturing of pyrite grains, ductile movement of chalcopyrite and gold, and pyrite recrystallization.

Electroplating of gold onto pyrite and chalcopyrite is common (Gilles and Bancroft, 1985). Gold found as inclusions in pyrite may represent gold electroplated onto pyrite surfaces or as gold injected into fractures by ductile deformation. Later recrystallization caused gold to be enveloped by pyrite. Thus, the precipitation of gold as free grains and electroplatings from hydrothermal solutions and the subsequent mechanical remobilization due to the Larder

Lake Break have given the deposit its present characteristics.

Plate 6: RX68000. Gold (G) in an intergranular setting between pyrite (Py). Magnetite (Mt) is found along pyrite grain boundaries. Field of view is 470  $\mu\text{m}$ . (PP). (320X).

Plate 7: RX67996. Gold inclusion in pyrite (Py) and gold (G) plating on pyrite. Field of view is 470  $\mu\text{m}$ . (PP). (320X).

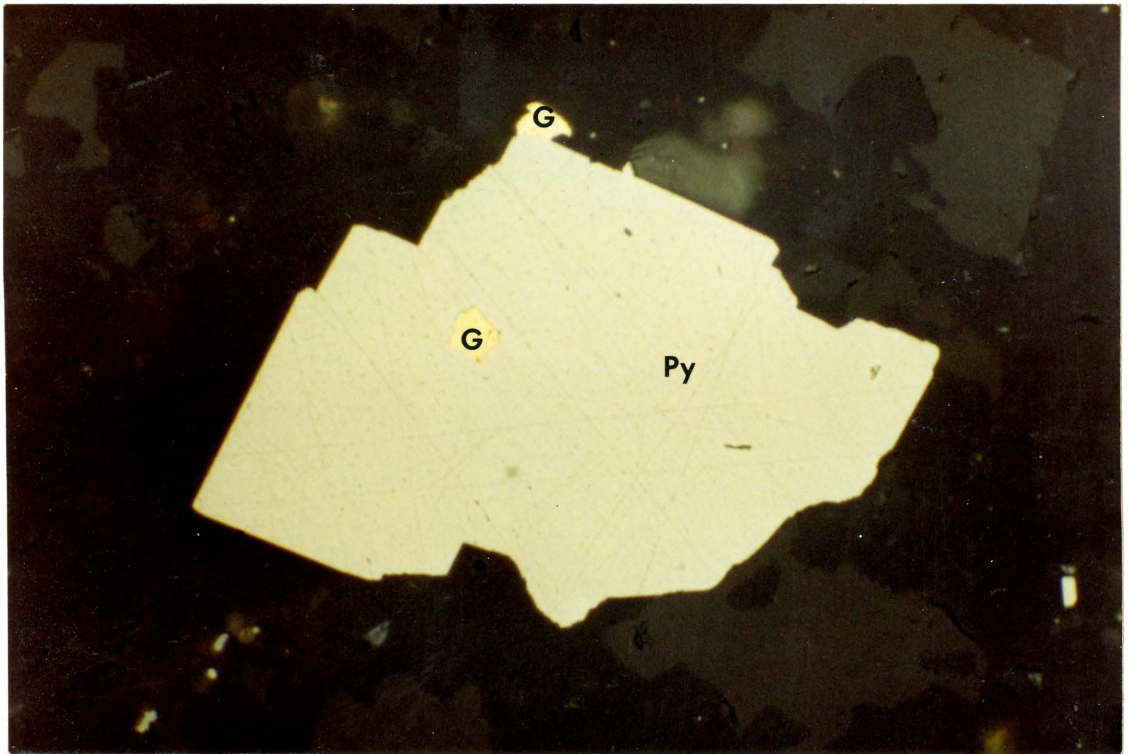
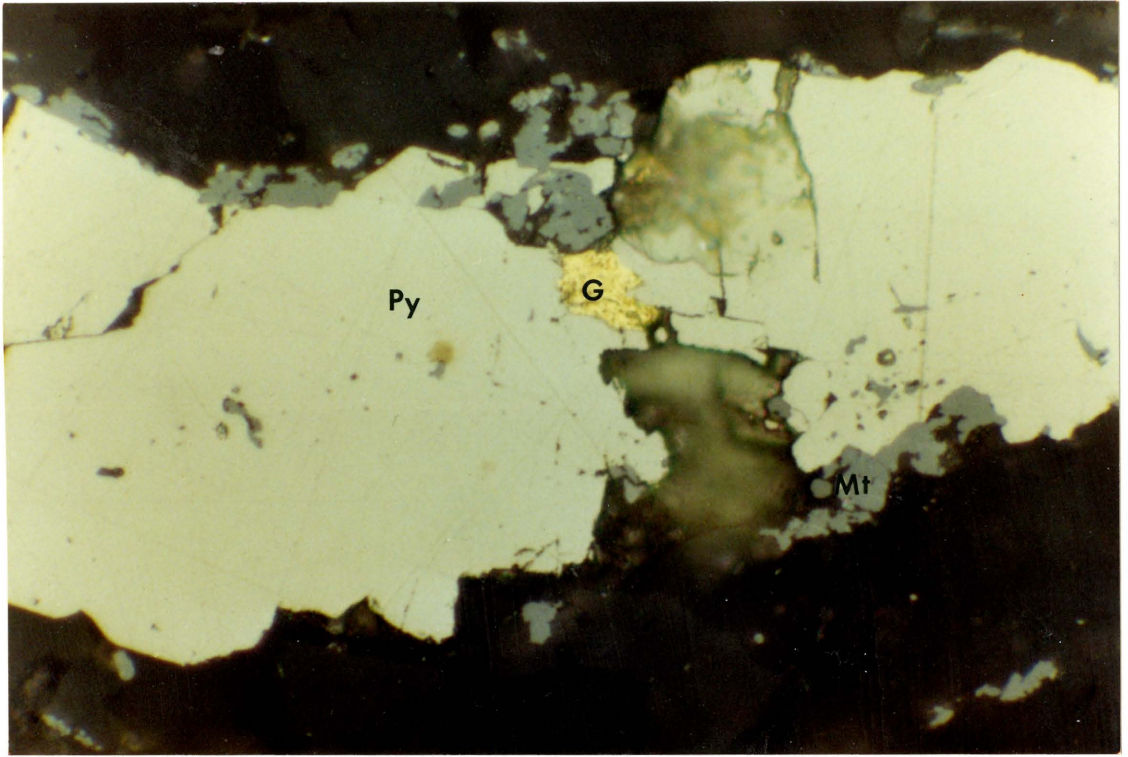


Plate 8: RX68000. Gold (G) plating on pyrite (Py).  
Adjacent grains are ilmenite (Il) and magnetite  
(Mt). Field of view is 190  $\mu\text{m}$ . (PP). (800X).

Plate 9: RX68000. Free gold (G) grains in gangue. Field  
of view is 290  $\mu\text{m}$ . (PP). (512X).



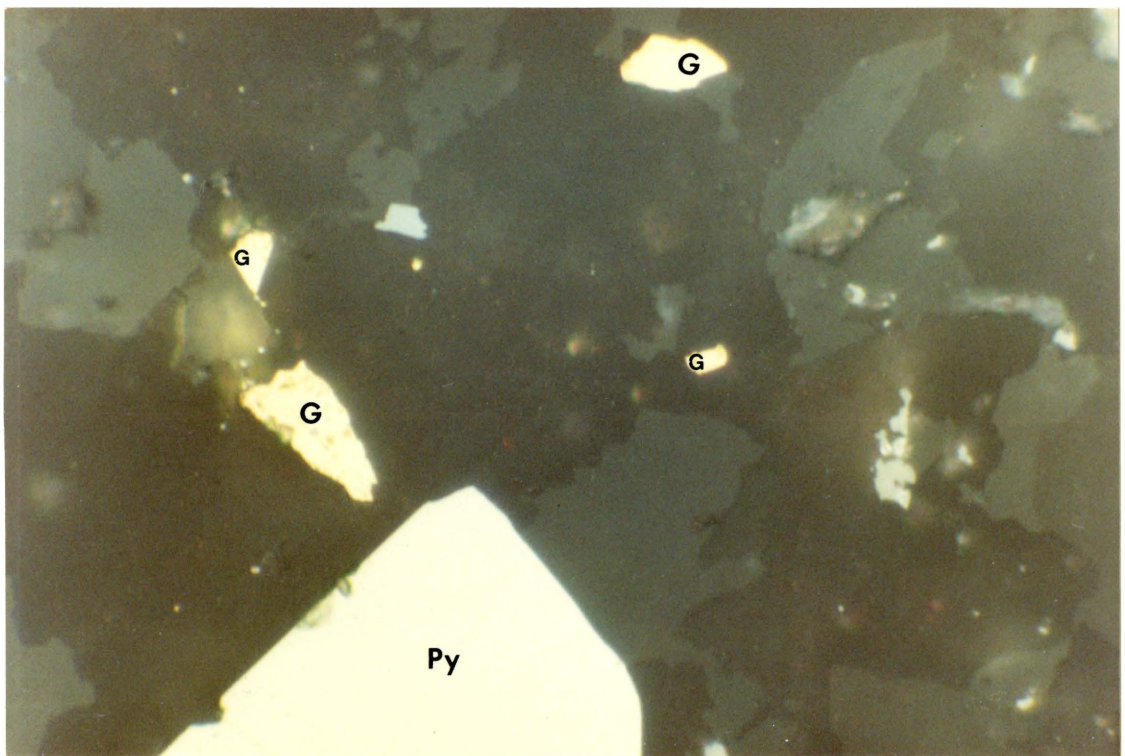
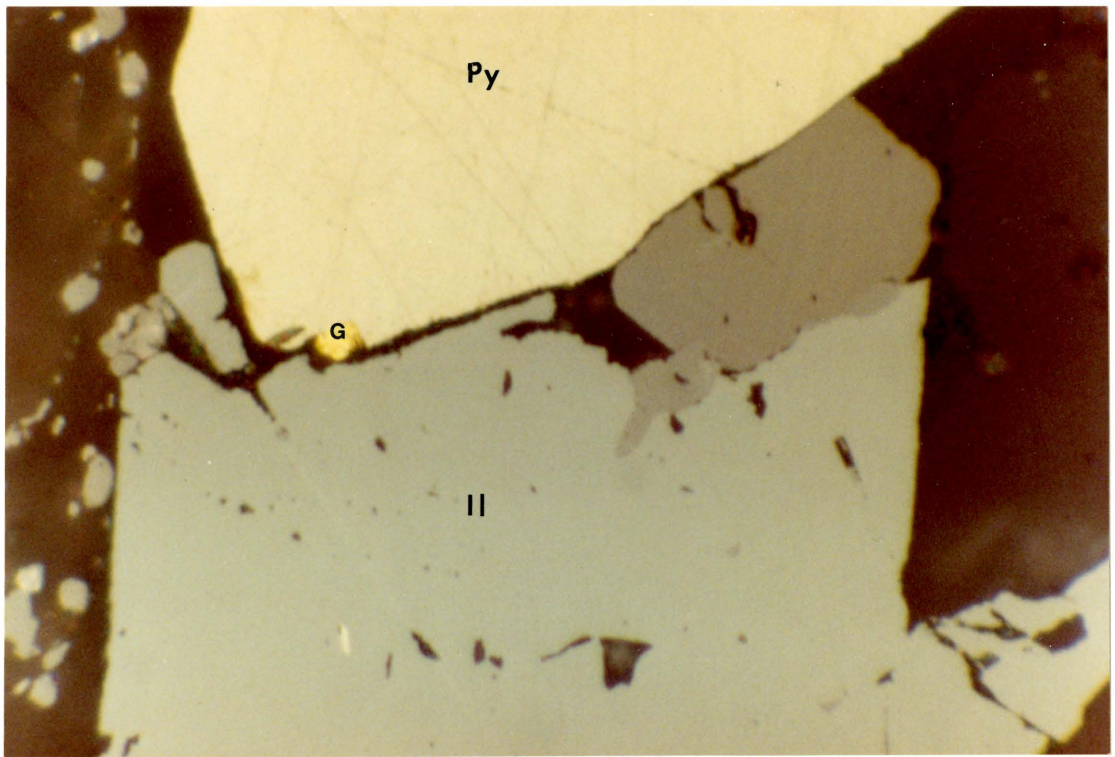


Plate 10: RX68000. Ilmenite (Il) exsolution from magnetite (Mt). Field of view is 730  $\mu\text{m}$ . (PP). (205X).

Plate 11: RX68000. Pyrite (Py) replacing magnetite (Mt). Field of view is 1.5 mm. (PP). (100X).



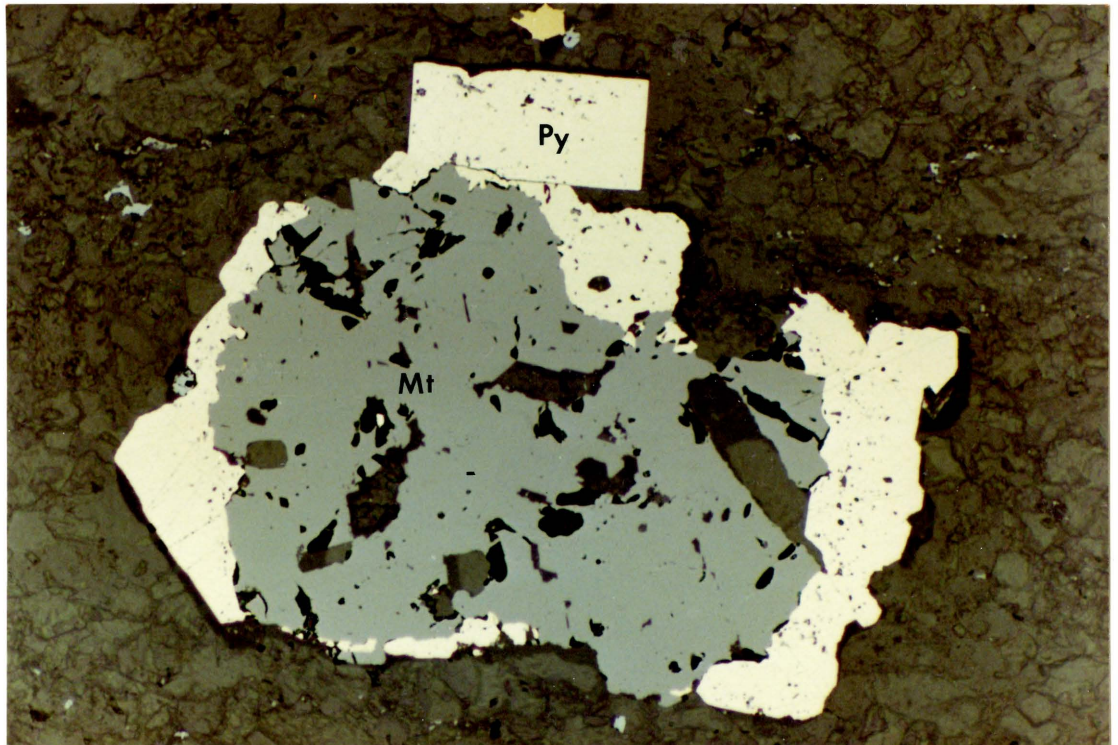
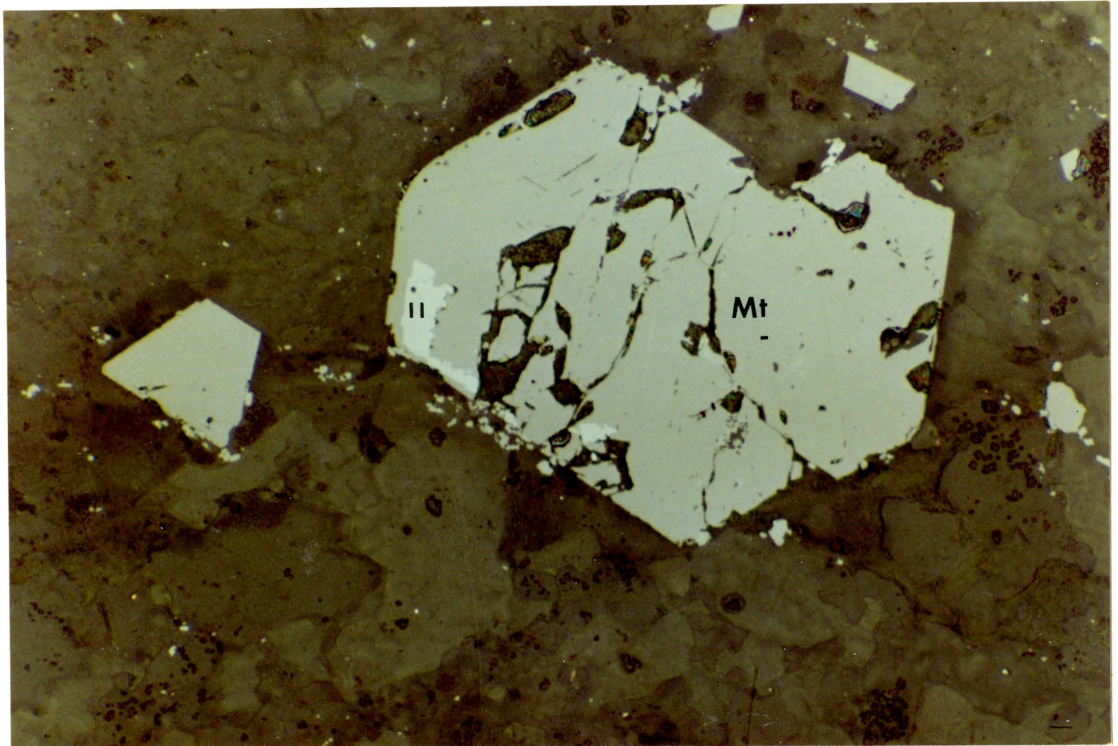


Plate 12: RX68000. Gold (G) plating on pyrite (Py) and chalcopyrite (Cp). Ilmenite (Il) and magnetite (Mt) also present. Field of view is 290  $\mu\text{m}$ . (PP). (510X).

Plate 13: RX68000. Gold (G) inclusion in pyrite (Py). Magnetite (Mt) with tiny chalcopyrite (Cp) inclusions is seen bordering pyrite. Field of view is 470  $\mu\text{m}$ . (PP). (320X).



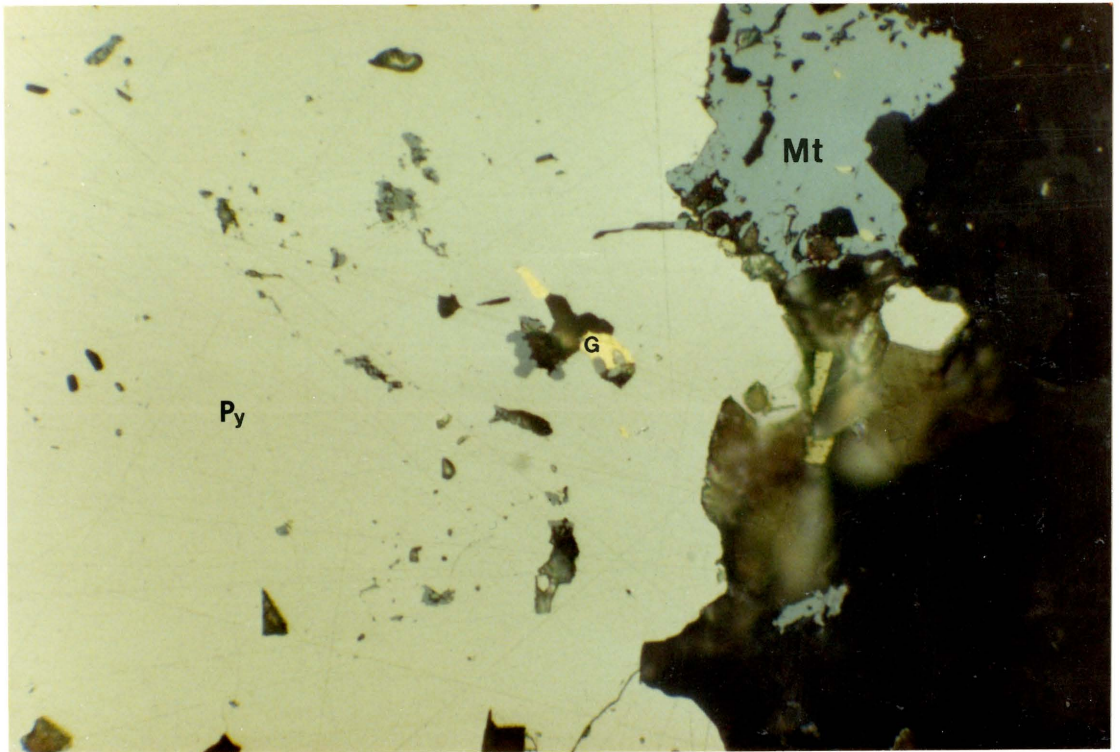
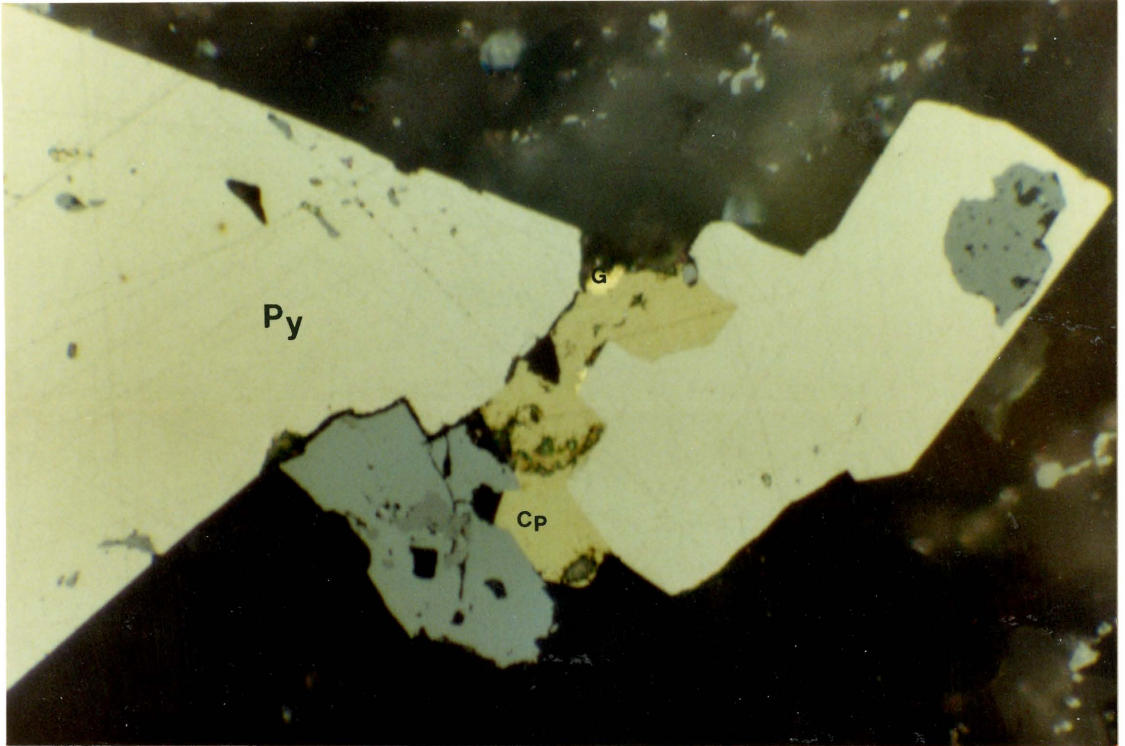
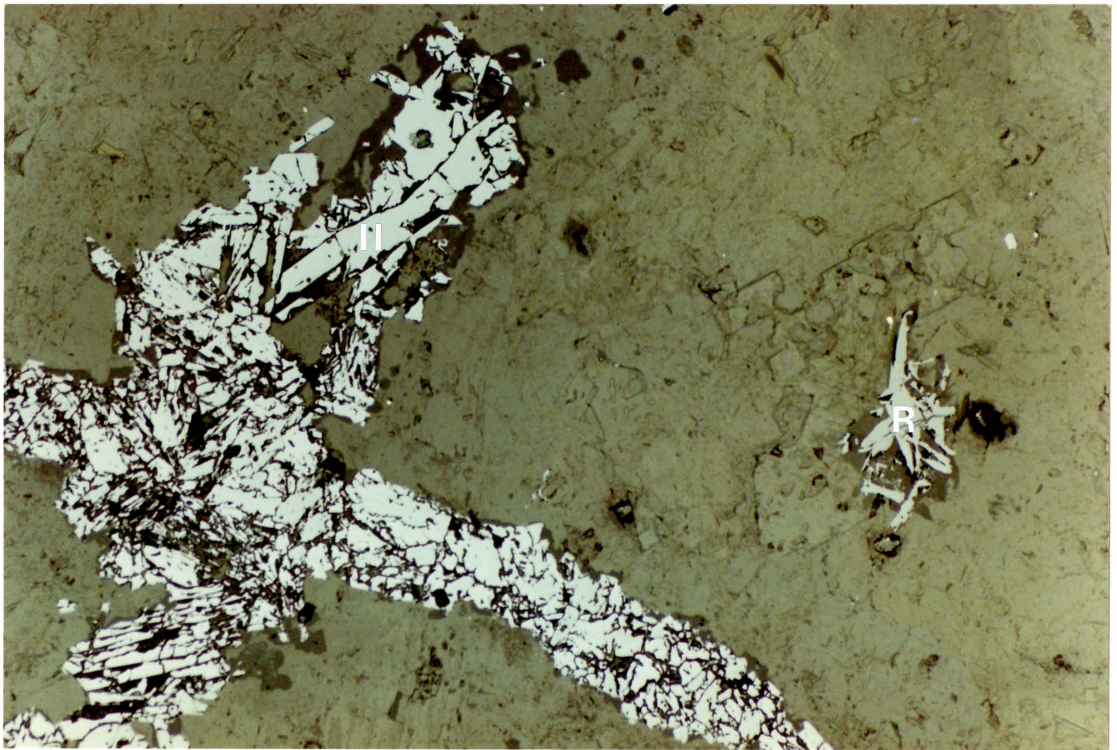
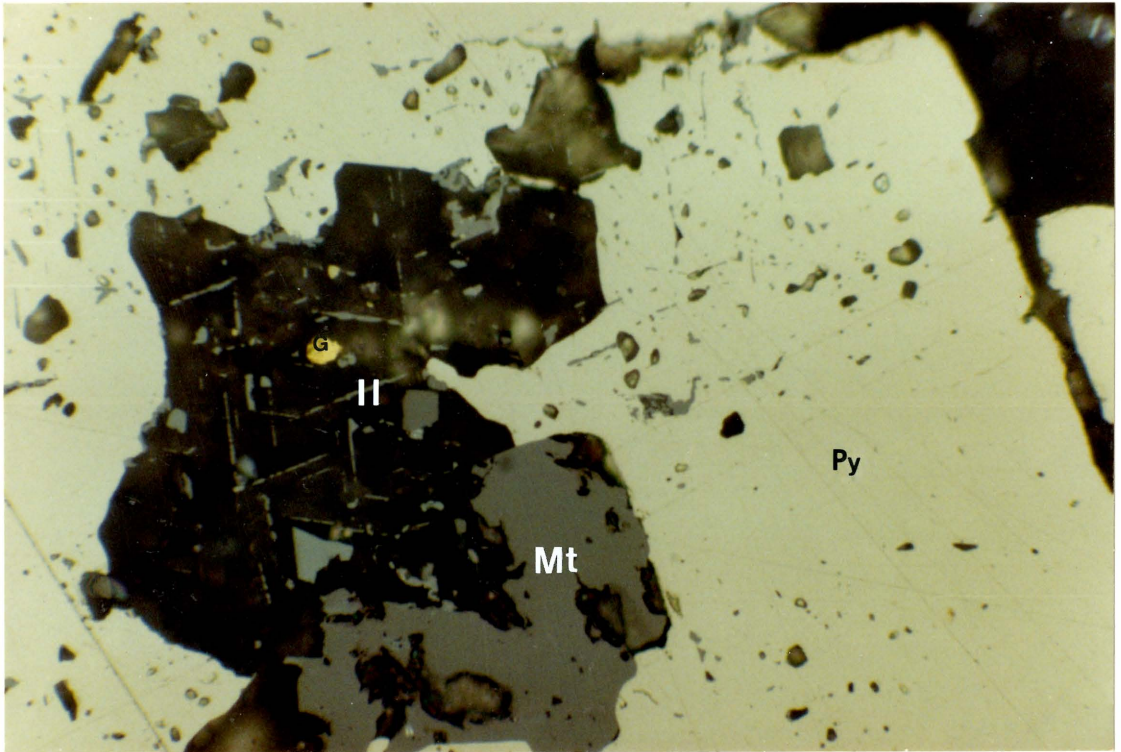




Plate 14: RX68000. Relict ilmenite (Il) laths, magnetite (Mt) and gold (G) found in an inclusion in pyrite (Py). Field of view is 470  $\mu\text{m}$ . (PP). (320X).

Plate 15: Ilmenite (Il) veinlet beside aggregate of rutile (R) laths. Field of view is 2.3 mm. (PP). (64X).



## CHAPTER 4 CARBONATE MINERALOGY: XRD ANALYSIS AND SCANNING ELECTRON MICROSCOPY

Carbonate rich zones are common in gold deposits of the Kirkland Lake-Larder Lake area. Most previous work on the deposits of the Kirkland Lake-Larder Lake gold camp does not specify the type of carbonate present. These minerals are referred to simply as carbonate or as a carbonate type in quotation marks. The green fuchsite bearing carbonitized rock at Kerr Addison was referred to by Thomson (1943) as "dolomite". It can be assumed that he had some reservations as to what the exact carbonate was. Thomson (1943) also describes carbonate associated with the Queenston Mine as "dolomite". Tulley (1963) reported dolomite, ankerite and calcite to be present in alteration zones at the Upper Canada Mine. No identification methods were stated. More recently Ridler (1972) and Downes (1981) have referred to the carbonate minerals associated with Kirkland Lake-Larder Lake Break deposits simply as carbonate. Tihor (1978) reports dolomite, magnesite and possibly ankerite to be present in the Kirkland Lake-Larder Lake area with some correlation between the presence of magnesite and gold. These results were based on XRD analyses.

From the XRD performed on McBean Mine samples dolomite and calcite were positively identified. Ankerite was not positively identified. Ankerite is referred to in this case as the end member of the dolomite-ankerite solid solution



series with a Mg:Fe ratio of <4. The primary peak of ankerite is too close to that of dolomite for the two to be distinguished. The main secondary peaks of ankerite were not present. Minerals identified by XRD are shown in the table below.

	<u>Dol.</u>	<u>Cal.</u>	<u>Ank.</u>	<u>Sid.</u>	<u>Alb.</u>	<u>Micro.</u>	<u>Or.</u>	<u>Talc</u>	<u>Chl.</u>	<u>Py.</u>
RX67899	*	-	?	-	-	*	-	*	*	-
RX68000	*	*	?	?	-	*	*	-	*	*
RX67980	*	*	?	-	*	-	*	*	*	*
RX67974	*	*	?	-	*	-	*	-	-	*

\*=present

-=not present

?=may be present

This analysis shows all samples to contain dolomite. The syenitic samples RX68000, RX67980 and RX67974 are enriched in gold values. These samples were shown to contain some calcite along with the dolomite. The peak intensities for calcite were weaker than for dolomite compared with their theoretical intensities. This implies that calcite is present in smaller amounts than dolomite. Thus, auriferous syenitic rocks are shown to contain dolomite with minor calcite while the non-auriferous talc-chlorite schist contains only dolomite.

Use of the SEM allowed for the comparison of the relative proportions of cations present in one carbonate grain to another. Points within the same grain can also be compared. The relative ratios of the counts at a particular

energy for Ca, Mg, Fe in carbonate grains from McBean samples are as follows:

<u>Sample</u>	<u>Ca:Fe:Mg Ratio</u>
RX67980,A	10.1:1.04:1
RX67971,B	10.2:1.2:1
RX67973,Ci (carbonate lining of quartz vein)	12.4:1.3:1
RX67973,Cii (carbonate veinlet)	7.5:1.2:1
RX67899,D (average)	7.7:0.5:1

These ratios differ greatly from the actual proportion of Ca to Mg in these carbonates, but, these relative ratios do yield some interesting information. Ternary diagrams with cation proportions normalized to 100% are shown in Figures 5 and 6. Plates 16 to 25 show the SEM electron image, analysis locations and an accompanying transmitted light photograph. The X-ray emissions from each location analysed can be found in Appendix 2.

Sample RX67899(D) is from talc-chlorite schist south of the ore zone. The carbonate grains in this rock were determined to dolomite by XRD. What were initially thought to be compositional lamellae can be seen in a carbonate grain in Plate 25. Analyses were made in the lamellae and outside the lamellae. Figure 5 shows the range of composition of the carbonate at the analysis locations. The iron content stays relatively constant, but, variations occur in Ca and Mg relative proportions. This variation between Ca and Mg occurs within the lamellae and outside the lamellae. On the



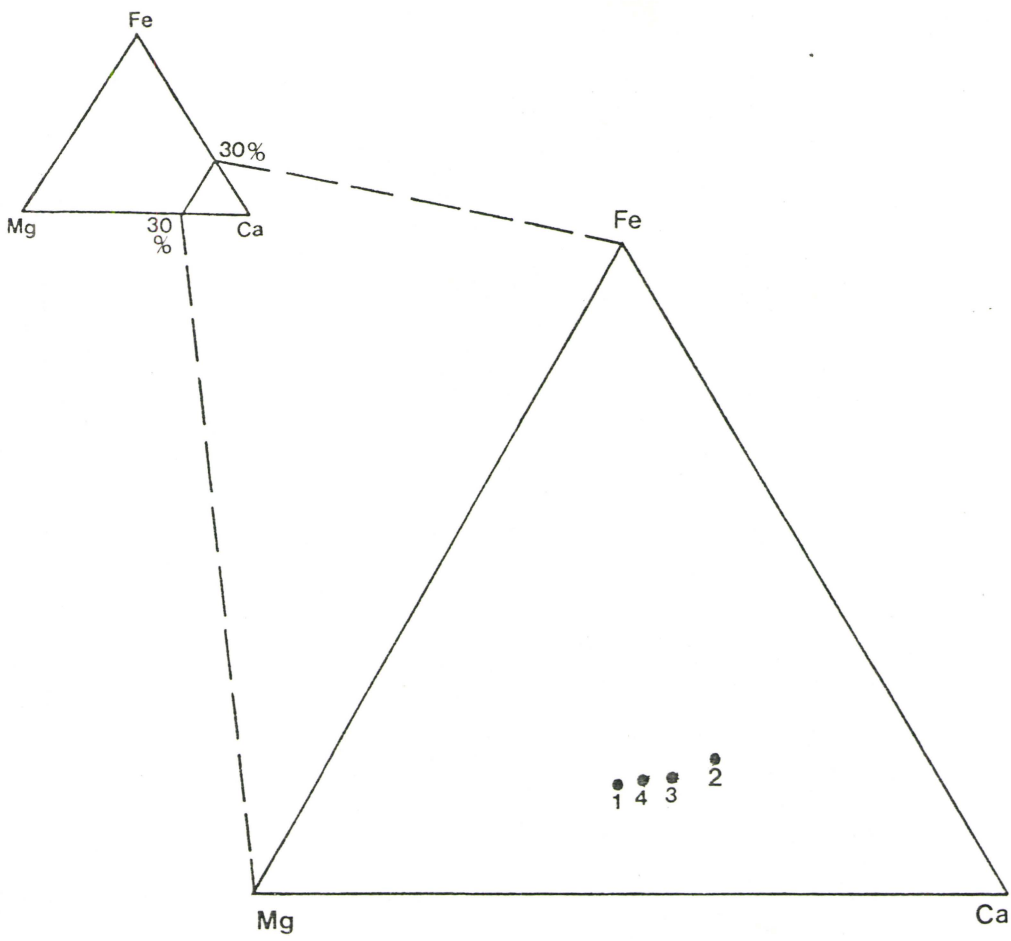


FIGURE 5 Relative Proportions of Carbonate Cation Counts at Common Energy Levels in Sample RX67899

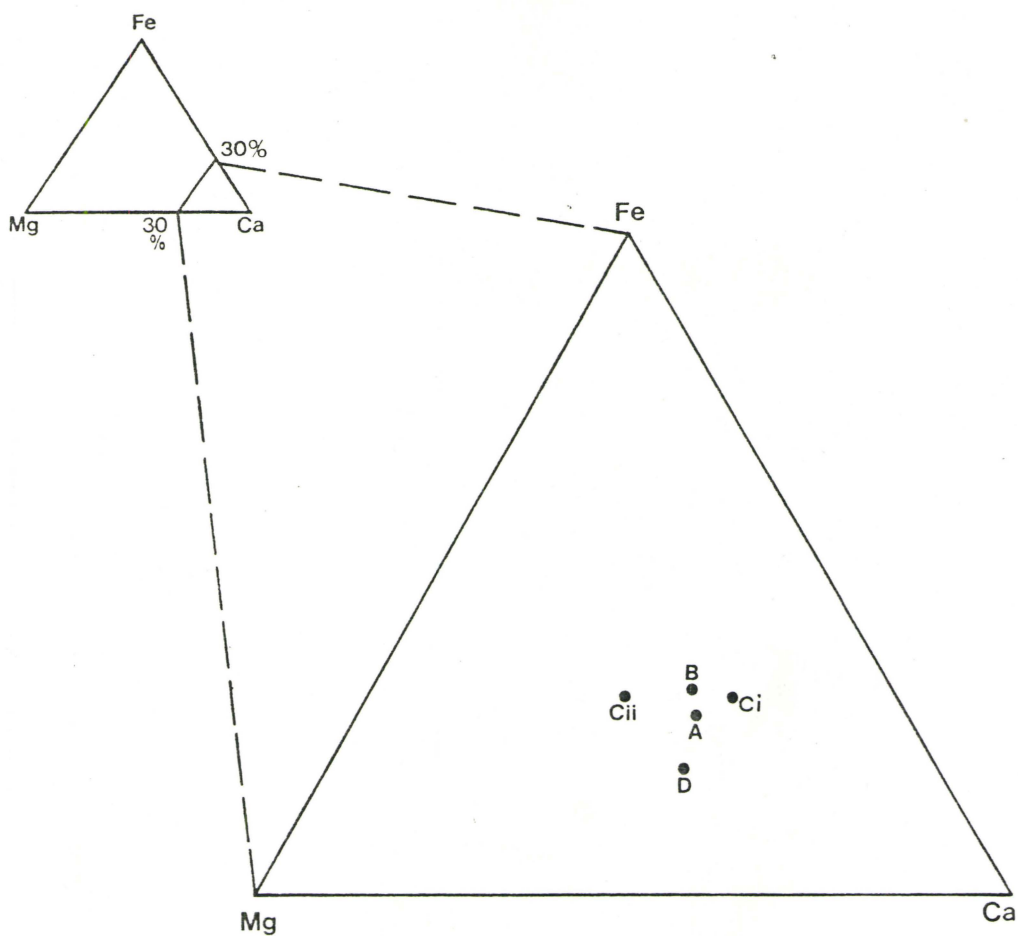


FIGURE 6 Relative Proportions of Carbonate Cation Counts at Common Energy Levels

A= RX67980 massive syenite

B= RX67971 gneissic syenite

Ci= RX67973 carbonate lining of quartz veinlet in syenite

Cii= RX67973 carbonate veinlet in syenite

D= RX67899 average of carbonate in talc-chlorite schist

average the lamellae are enriched in the relative proportion of Ca and depleted in Mg. Thus, these lamellae have an average composition which is different from the rest of the grain. An alternate, considered less likely in view of the above is that the lamellae may be due to crystallographic twinning.

Figure 6 is a plot of the average composition of the carbonate in RX67899 and in three other samples. This diagram shows that the carbonate in the talc-chlorite schist sample (RX67899) is depleted in its proportion Fe relative to Ca and Mg compared with the syenitic rocks. The carbonate grains from the massive syenite sample (RX67980) and the gneissic syenite sample (RX67971) have very similar proportions of Fe, Ca and Mg. Sample RX67980 has a gold assay of 1.21 ppm while sample RX67971 has an assay of <5 ppb. Judging from this data there does not appear to be a correlation between the relative proportions of cations in non-vein carbonate grains and gold values.

To see if carbonate grains found in veinlet systems have similar compositions, a syenite sample (RX67973) from the ore zone containing vein carbonate was examined. In this sample carbonate grains were analysed from the carbonate lining of a quartz vein and from a carbonate veinlet. The carbonate veinlet was found to have a greater relative proportion of Mg than the carbonate vein lining and the other samples analysed. The carbonate vein lining was in turn more rich in its relative proportion of Ca compared to the carbonate

veinlet and the other samples. These compositions are plotted on Figure 6. This implies that carbonate rich solutions of varying composition were injected along fractures in the syenite at different times. Thus, the gold mineralization could be associated with a specific type of vein carbonate. Analysing the carbonate in a suite of samples from across the ore zone with a microprobe could resolve this.

The SEM was also useful in confirming the presence of minerals examined in thin sections and polished thin sections. Besides carbonate the SEM aided in the identification of plagioclase (albite), K-spar, apatite, pyrite and ilmenite.

Plate 16: RX67980. Backscatter Electron Image of ilmenite veinlet. Cb=carbonate, Il=ilmenite, Pg=plagioclase. Bar=100 um. (143X).

Plate 17: RX67980. Transmitted light, photomicrograph of area in Plate 16. Field of view is 1.5 mm. (XP).



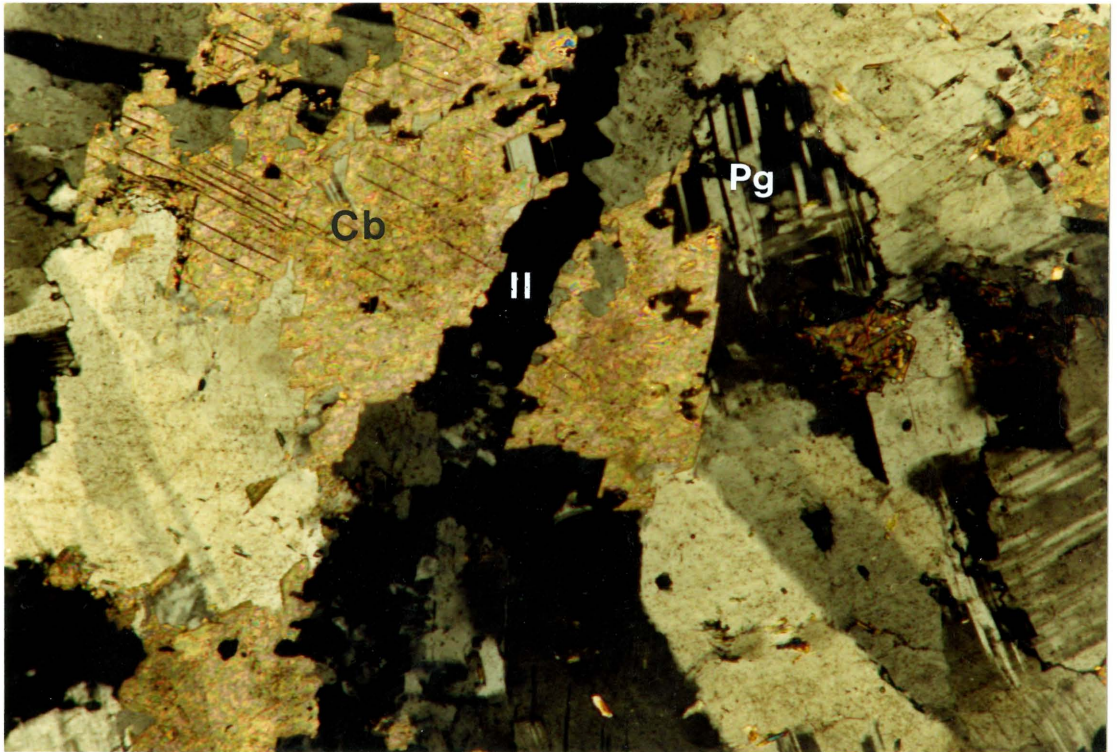
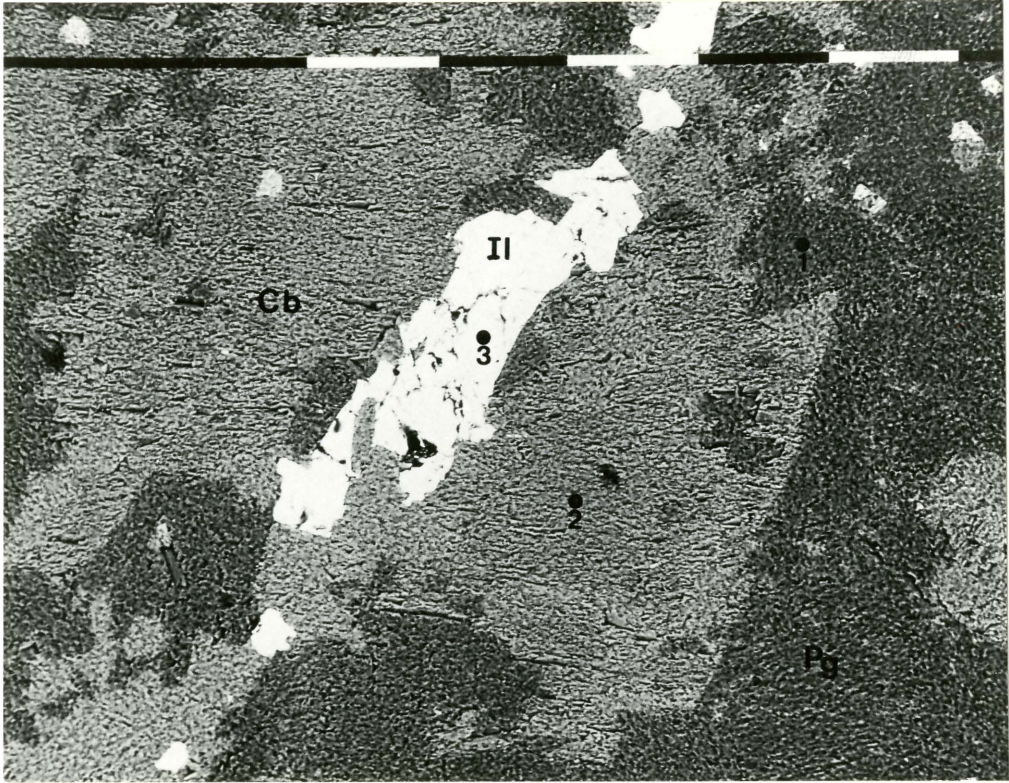


Plate 18: RX67971. Backscatter Electron Image. Py=  
pyrite, Cb=carbonate, K-sp=potassium feldspar.  
Bar=1 mm. (71.5X).

Plate 19: RX67971. Transmitted light photomicrograph of  
area in plate 18. Field of view is 6 mm. (XP).



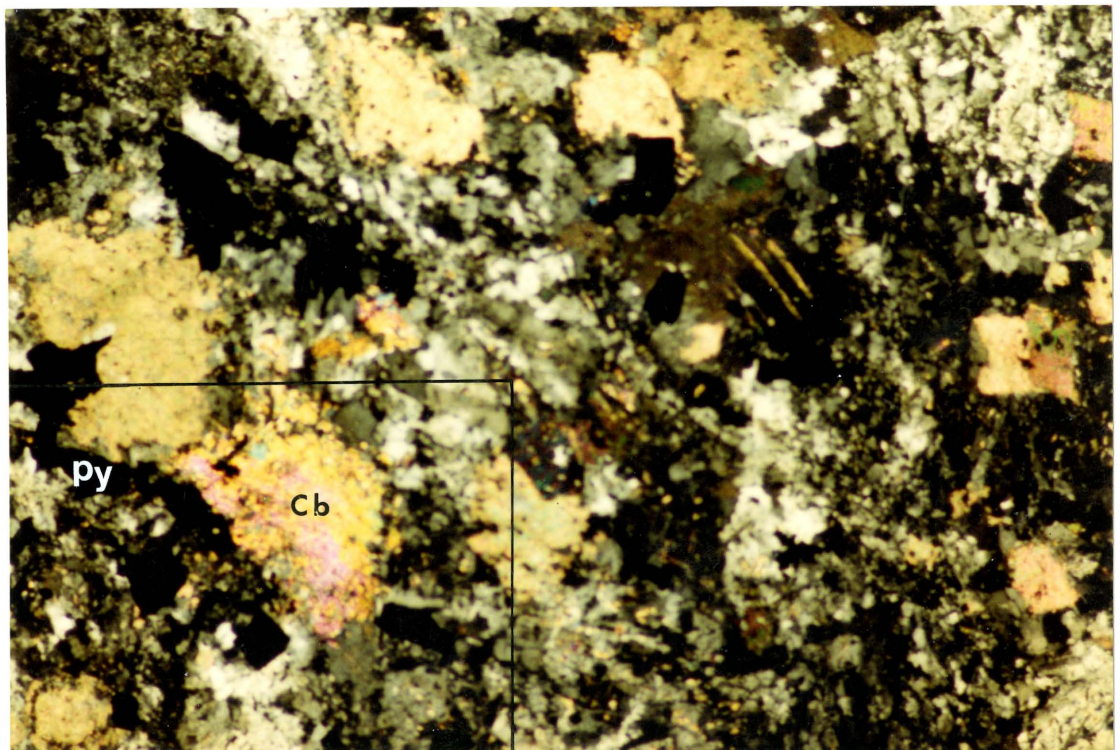
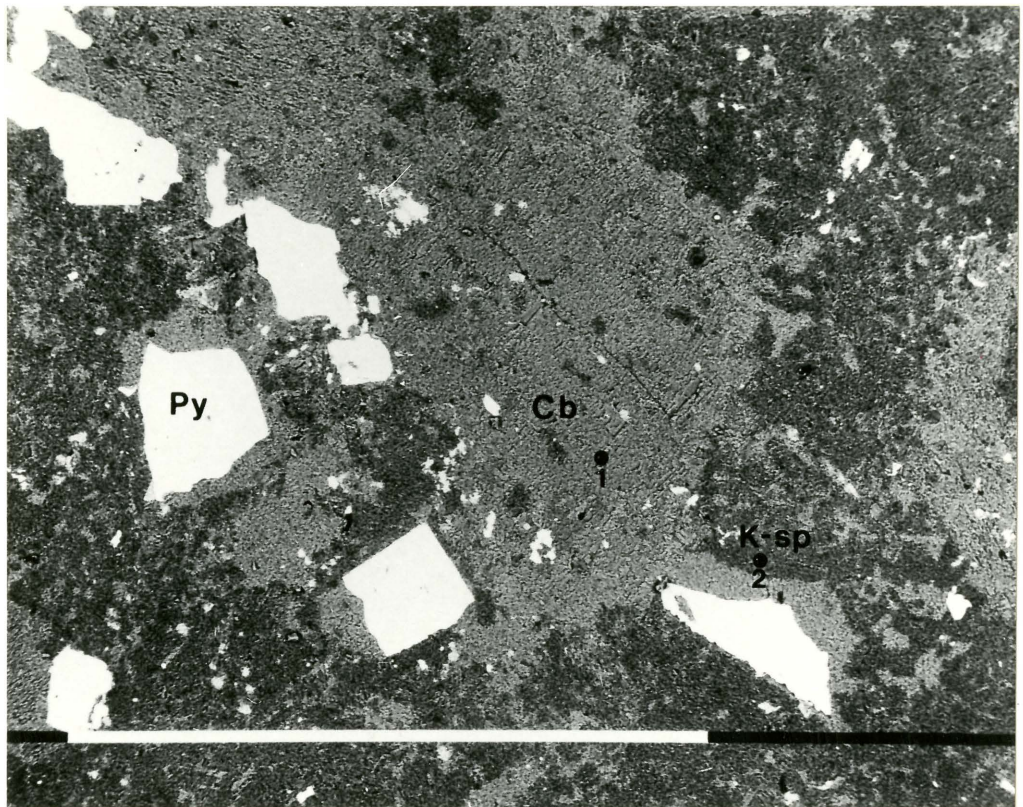


Plate 20: RX67973,Cii. Backscatter Electron Image of carbonate veinlet. Cb=carbonate, Py=pyrite, Pg=plagioclase, K-sp=potassium feldspar, Ap=apatite. Bar=1 mm. (31.4X).

Plate 21: RX67973,Cii. Transmitted light photomicrograph of area in Plate 20. Field of view is 6 mm. (XP).



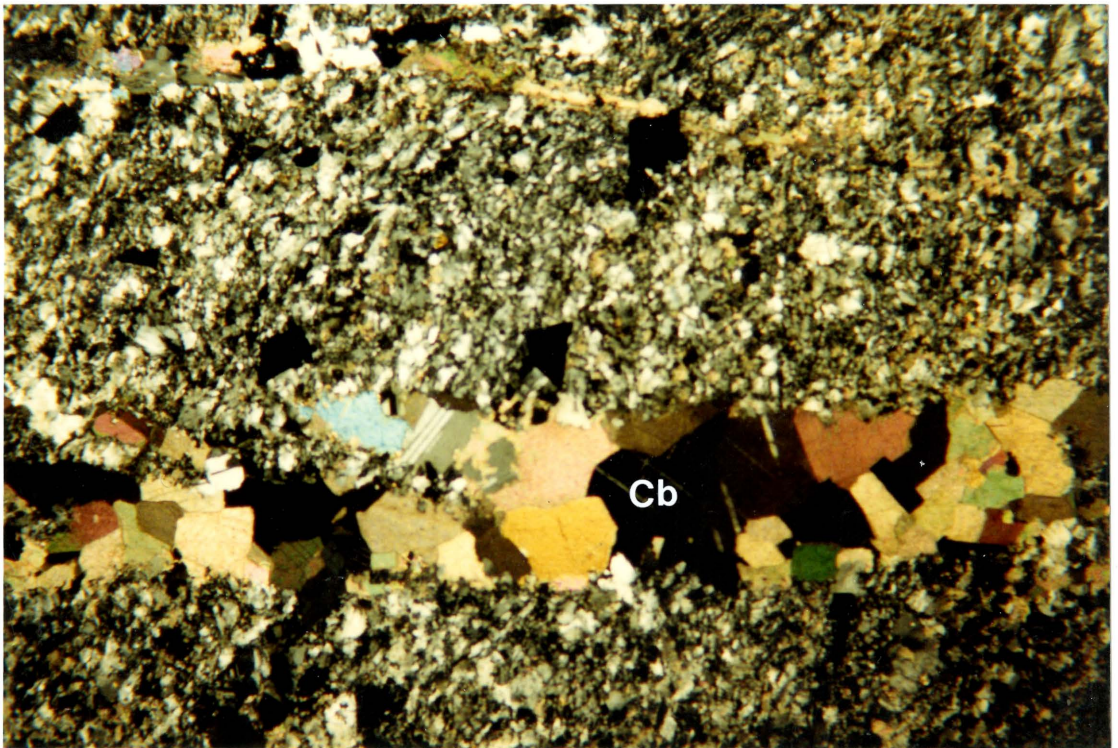
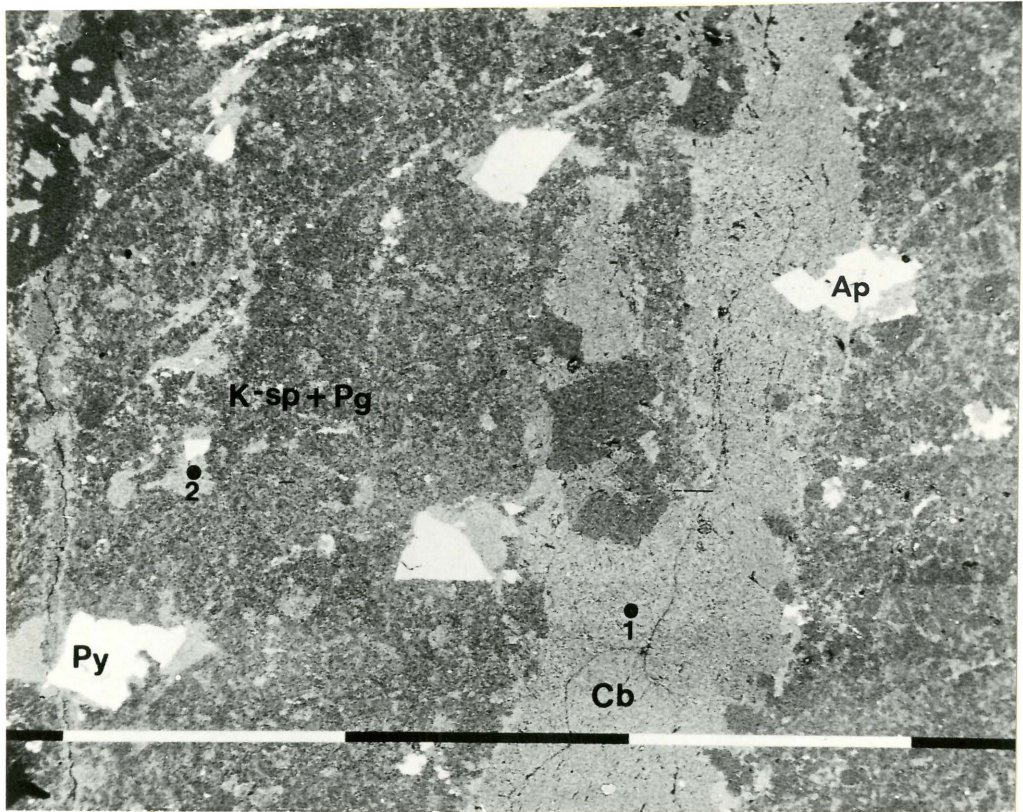


Plate 22: RX67973, Ci. Backscatter Electron Image of carbonate lining a quartz veinlet. Qtz=quartz, Cb=carbonate, Py=pyrite, Pg=plagioclase, K-sp=potassium feldspar. Bar=1 mm. (32.8X).

Plate 23: RX67973,Ci. Transmitted light photomicrograph of area in Plate 22. Field of view is 4 mm. Image is inverted. (XP).



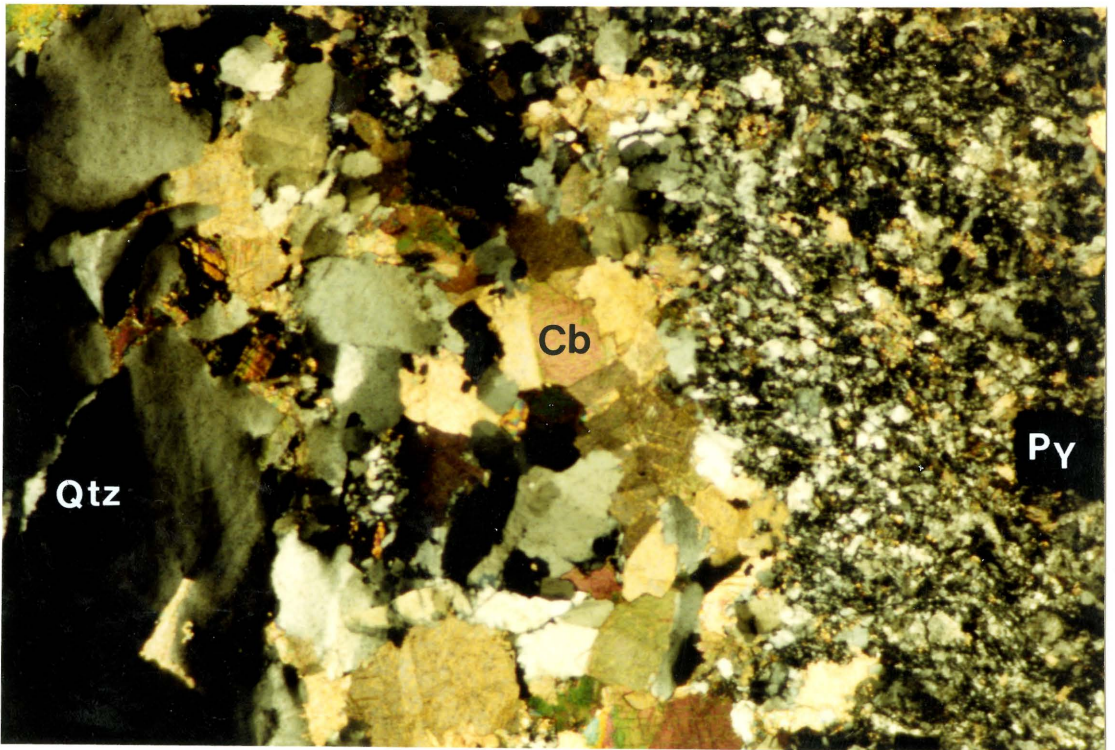
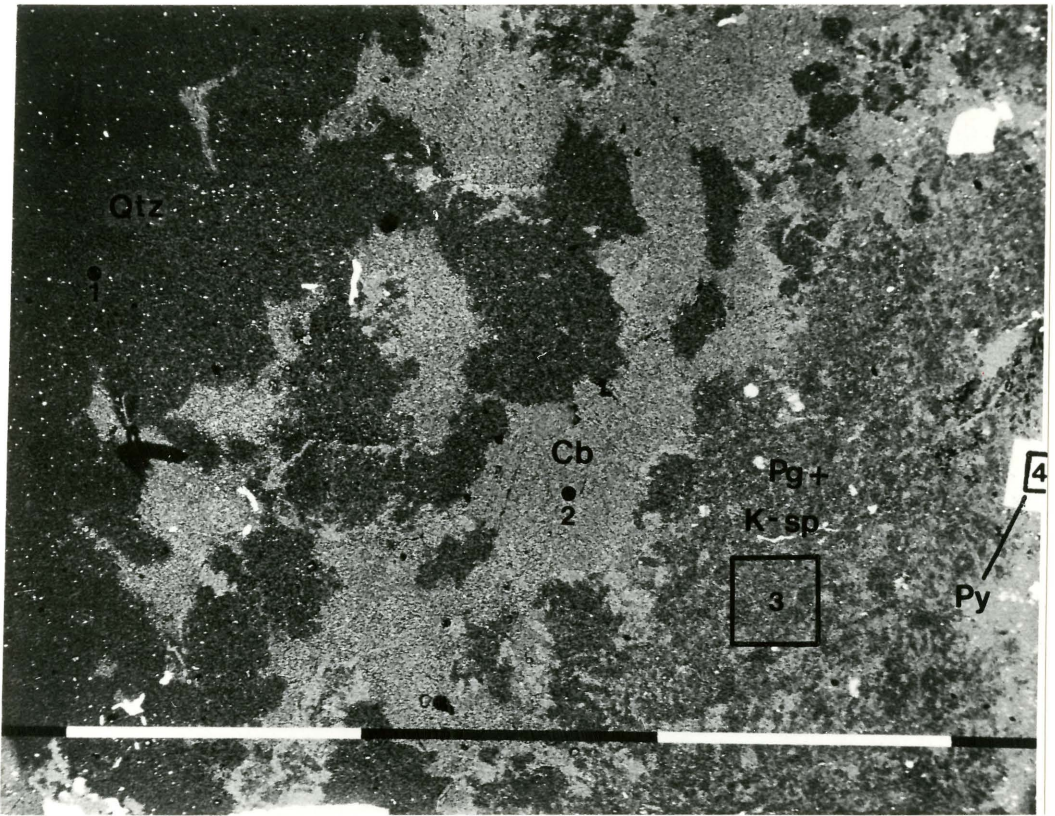


Plate 24: RX67899. Secondary Electron Image.

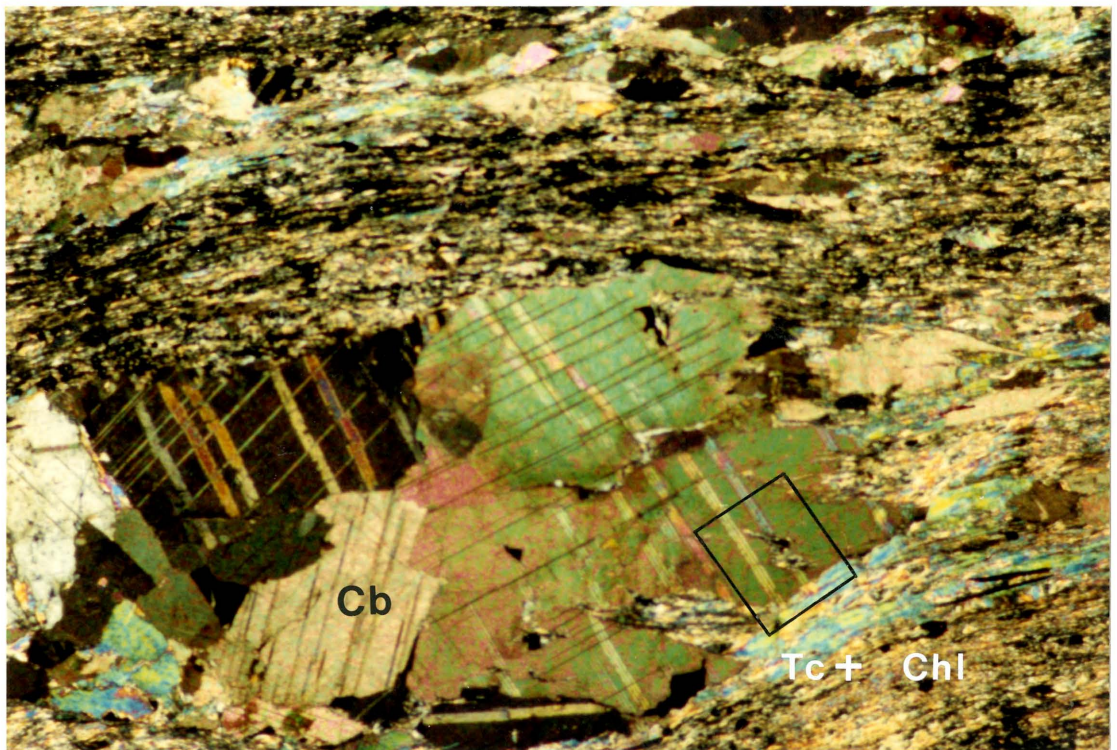
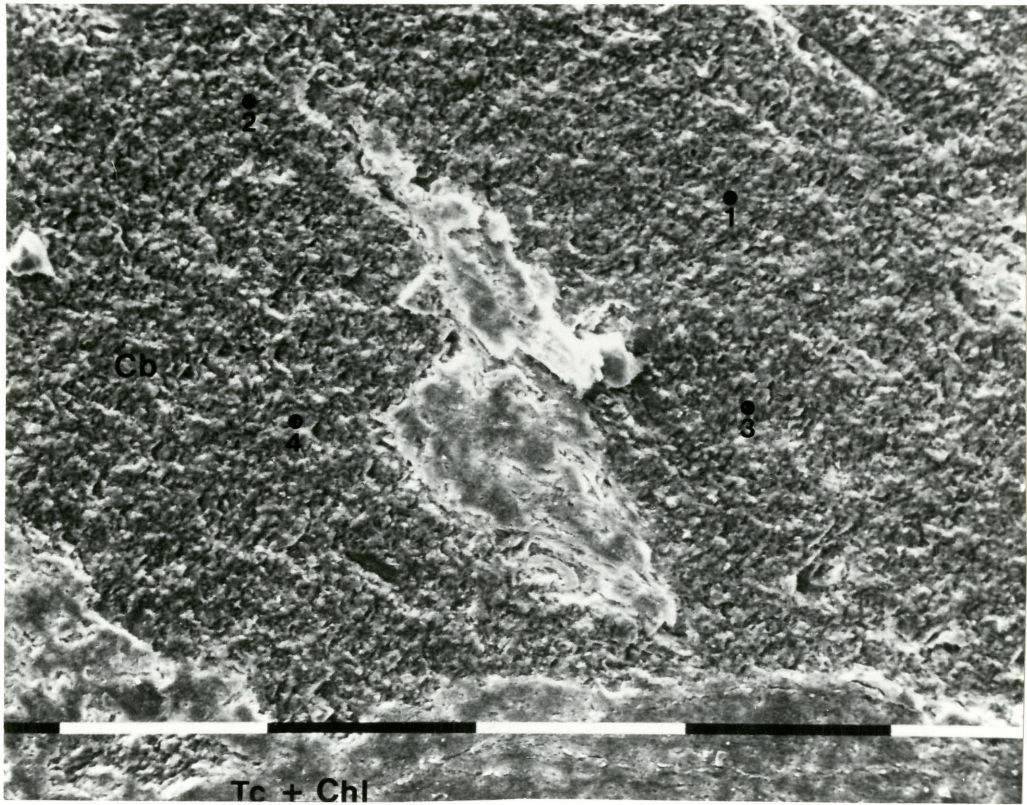
Cb=carbonate, Tc=talc, Chl=chlorite. Bar=100 um.

(231X).

Plate 25: RX67899. Transmitted light photomicrograph of

area in Plate 24. Field of view is 4 mm. (XP).





## CHAPTER 5 GEOCHEMISTRY

### 5.1 Bulk Composition

The XRF analyses of the major elements can be found in Table 1. Analyses are presented for each rock type from south of the ore zone, through the ore zone into gneissic syenite bands north of the ore zone. The sample locations are shown in Fig. 3. An approximation of the degree of alteration in these rocks is shown by the LOI abundances. The least altered rocks are the massive syenites in the ore zone. These rocks display an LOI abundance of approximately 6 wt.%. The most altered rock in the pit area is the talc-chlorite schist. This unit has an LOI abundance of approximately 19 wt.% due mainly to high carbonate content. The mafic syenite units display a high degree of alteration as well with an LOI abundance of approximately 16 wt.%. The alteration in these units is due to their proximity to the intrusive syenites and hydrothermal alteration processes.

Gneissic syenite samples have approximately double the LOI value of the massive syenites. The gneissic syenites therefore appear to be much more altered than the massive syenites. This is due to increased hydrothermal carbonate alteration and closer proximity to the Larder Lake Break. The assumption that the degree of alteration varies closely with LOI is validated by the amount of carbonate in the two rock types. The gneissic syenites contain a much greater



Table 1. Major Element Abundances and Normative Minerals

	RX67899	RX67973	RX67974	RX67975	RX67976
SiO <sub>2</sub>	32.30	62.38	68.41	39.85	38.83
Al <sub>2</sub> O <sub>3</sub>	3.58	12.04	13.86	8.81	7.68
Fe <sub>2</sub> O <sub>3</sub>	9.45	4.42	3.24	8.96	7.64
MgO	25.66	2.39	2.45	11.32	14.35
CaO	9.39	4.57	2.39	10.17	9.39
Na <sub>2</sub> O	0.06	4.05	4.26	0.66	0.47
K <sub>2</sub> O	0.18	2.40	1.03	2.51	4.18
TiO <sub>2</sub>	0.21	0.18	0.01	0.17	0.12
P <sub>2</sub> O <sub>5</sub>	0.11	0.22	0.11	0.34	0.30
LOI	18.87	7.13	3.97	16.67	16.54
CO <sub>2</sub>	15.52	7.22	5.85	16.83	16.02
H <sub>2</sub> O	3.35	0.0	0.0	0.0	0.52
-XRF analysis in wt.%					
CIPW NORMS					
ct	16.6	7.6	3.9	17.4	16.1
mg	16.0	5.0	5.0	17.7	17.3
sd	0.0	3.4	1.8	0.0	0.0
ap	0.3	0.5	0.3	0.8	0.7
il	0.4	0.6	0.5	1.0	1.0
or	1.1	14.2	6.0	14.9	24.8
ab	0.5	34.3	27.0	5.6	4.0
C	3.3	2.8	7.3	5.0	2.4
mt	2.5	0.0	0.0	3.0	2.9
hm	0.0	1.8	1.7	0.0	0.0
qz	0.0	29.7	44.9	18.0	7.8
ol	2.2	0.0	0.0	0.0	0.0
fo	1.7	0.0	0.0	0.0	0.0
fa	0.5	0.0	0.0	0.0	0.0
hy	53.8	0.0	0.0	16.5	22.5
en	42.9	0.0	0.0	7.2	15.4
fs	10.8	0.0	0.0	9.3	7.1
Au Fire Assay	<5 ppb	320 ppb	900 ppb	45 ppb	<5 ppb
Rock Type	Talc Chlorite Schist	Massive Syenite	Massive Syenite	Banded Mafic Syenite	Mafic Syenite

\* note mg=magnesite sd=siderite

Table 1. cont'd

	RX67980	RX67982	RX67993	RX67996	RX68000
SiO <sub>2</sub>	56.92	42.57	55.60	46.39	37.78
Al <sub>2</sub> O <sub>3</sub>	16.77	11.66	11.04	14.48	10.46
Fe <sub>2</sub> O <sub>3</sub>	6.45	10.51	6.11	10.35	14.93
MgO	1.44	8.24	4.22	5.32	6.95
CaO	3.67	8.47	6.21	6.64	10.48
Na <sub>2</sub> O	6.15	2.04	2.64	2.97	0.72
K <sub>2</sub> O	2.27	2.11	2.16	2.24	2.62
TiO <sub>2</sub>	0.30	0.73	0.33	0.57	0.84
MnO	0.09	0.16	0.12	0.13	0.20
P <sub>2</sub> O <sub>5</sub>	0.34	0.46	0.36	0.63	1.18
LOI	5.59	13.05	11.22	10.58	13.84
CO <sub>2</sub>	5.58	12.83	10.22	9.94	10.80
H <sub>2</sub> O	0.01	0.22	1.00	0.64	3.04
-XRF analysis in wt.%					
CIPW NORMS					
ct	5.8	14.2	10.3	10.5	16.1
mg	3.0	12.9	8.9	10.4	7.4
sd	3.9	0.0	2.9	0.0	0.0
ap	0.8	1.1	0.8	1.5	2.8
il	0.6	1.4	0.6	1.1	1.6
or	13.5	12.6	12.8	13.3	15.7
ab	52.3	17.4	22.4	25.3	6.17
C	4.2	6.1	4.4	6.9	6.5
mt	2.6	3.3	2.7	3.0	3.4
hm	0.0	0.0	0.0	0.0	0.0
qz	11.9	14.6	31.2	14.9	10.4
ol	0.0	0.0	0.0	0.0	0.0
fo	0.0	0.0	0.0	0.0	0.0
fa	0.0	0.0	0.0	0.0	0.0
hy	1.4	16.4	1.9	12.4	26.8
en	0.0	5.4	0.0	1.0	8.8
fs	1.4	11.0	1.9	11.4	18.0
Au Fire Assay	1.21 ppm	55 ppb	2.11 ppm	1.02 ppm	15.4 ppm
Rock Type	Massive Syenite	Dioritic Gneiss	Quartz Vein and Syenitic Rock	Gneissic Syenite	Gneissic Syenite



amount of carbonate (approx. 30% modal carbonate) than the massive syenites (5-10% modal carbonate).

As well as containing greater abundances of  $\text{CO}_2$  the Gneissic syenites have higher  $\text{CaO}$  and  $\text{MgO}$  contents which also reflects a greater degree of hydrothermal carbonate alteration. The gneissic syenites also display lower  $\text{SiO}_2$  levels than the massive syenites. Along the level 1 ramp gold is preferentially concentrated in narrow gneissic syenite bands which display a high degree of hydrothermal carbonate alteration. This variation in the degree of alteration is documented by the bulk compositions of the samples.

The average compositional range of typical syenite and felsic syenite from the Macassa Mine are shown in Table 2. The LOI and  $\text{CO}_2$  values for McBean syenites are lower double the values at Macassa. This is due to the a lesser degree of hydrothermal carbonate alteration occurring at Macassa. The McBean syenites also display low  $\text{K}_2\text{O}$  abundances. There is of course a dilution effect from high  $\text{CO}_2$ ,  $\text{CaO}$ ,  $\text{MgO}$  and  $\text{Fe}_2\text{O}_3$  values. These low  $\text{K}_2\text{O}$  values are reflected in the predominance of plagioclase over potassium feldspar in the McBean syenites.

The feldspar in the least altered syenite, sample RX67897, is dominantly plagioclase. This sample contains up to 30% plagioclase of albite composition. Another relatively unaltered sample, RX67980, which is from the ore zone was found to contain albite from an SEM analysis. Thus, the low

Table 2. Average Bulk Composition Range of Typical Syenite and Bulk Composition of Unaltered and Altered-Mineralized Felsic Syenite from Macassa Mine

	Typical Syenite*	Macassa Unaltered Felsic Syenite+	Macassa Altered and Mineralized Syenite+
SiO <sub>2</sub>	52-69.2	56.2	57.6
TiO <sub>2</sub>	0.1-1.3	0.6	0.5
Al <sub>2</sub> O <sub>3</sub>	15.4-23.1	18.9	19.5
Fe <sub>2</sub> O <sub>3</sub>	0.6-3.5	4.1	3.3
FeO	0.5-5.7		
MnO	0.05-0.3	0.1	0.04
MgO	0.1-2.0	0.1	0.6
CaO	1.1-3.5	1.9	1.1
K <sub>2</sub> O	3.3-8.8	7.5	9.9
P <sub>2</sub> O <sub>5</sub>	0.0-0.4	0.2	0.2
CO <sub>2</sub>	0.05-1.1	3.0	
LOI			3.0

-abundances in wt.%

\*from Hyndman, 1985

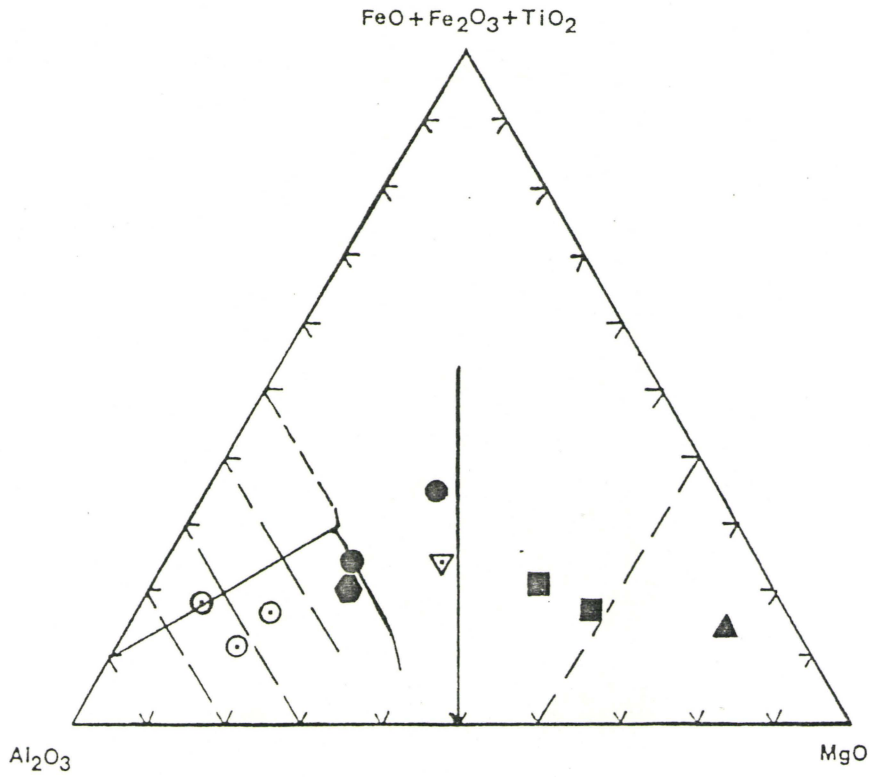
+from Kerrich and Watson, 1984

K<sub>2</sub>O abundance and the dominance of plagioclase over potassium feldspar suggests this rock may be transitional between a syenite and a monzonite. This rock may be a plagioclase rich variation of a parental intrusion. To be consistent these rocks will still be termed syenite for the remainder of this study.

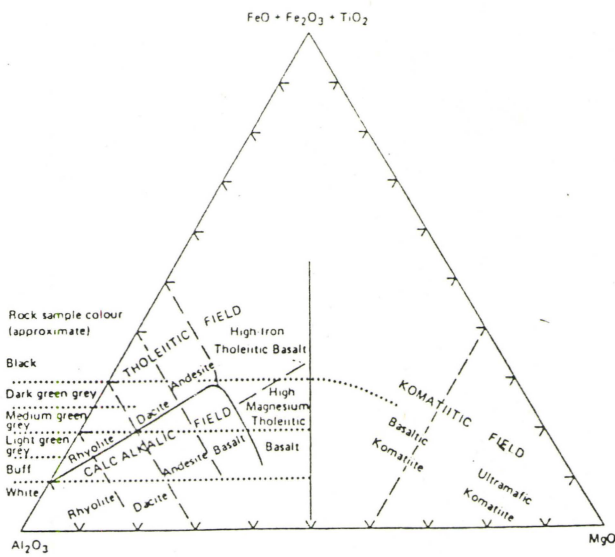
The analysed samples were plotted on a Jensen Cation Plot (see Fig.7). The talc-chlorite schist plots in the ultramafic komatiite field indicating that this rock is probably an altered komatiite. The magnesium rich character is reflected in the pervasive chlorite and talc seen in thin section. The mafic syenites plot in the basaltic komatiite field suggesting that they may be altered komatiitic basalts. In thin section these samples contain abundant biotite, carbonate, chlorite and very fine grained quartz. The gneissic syenites plot in the high iron tholeiitic field of the diagram. These intrusives have elevated Fe concentrations due to abundant pyrite. The high magnesium concentrations arise from the presence of dolomite and chlorite. The massive syenites fall in the calc-alkalic field as they contain more feldspar and less carbonate than the gneissic syenites. The calc-alkalic composition of these intrusives suggest that they were derived from the partial melting of sediments proximal to calc-alkalic volcanic rocks.

CIPW mineral norms were calculated using a modified computer program which calculates normative carbonate abundances as well as the usual normative minerals (program

Figure 7 Jensen Cation Plot



- gneissic syenite ●
- syenite ○
- talc chlorite schist ▲
- mafic syenite ■
- dioritic gneiss ▽
- quartz vein with syenite ●





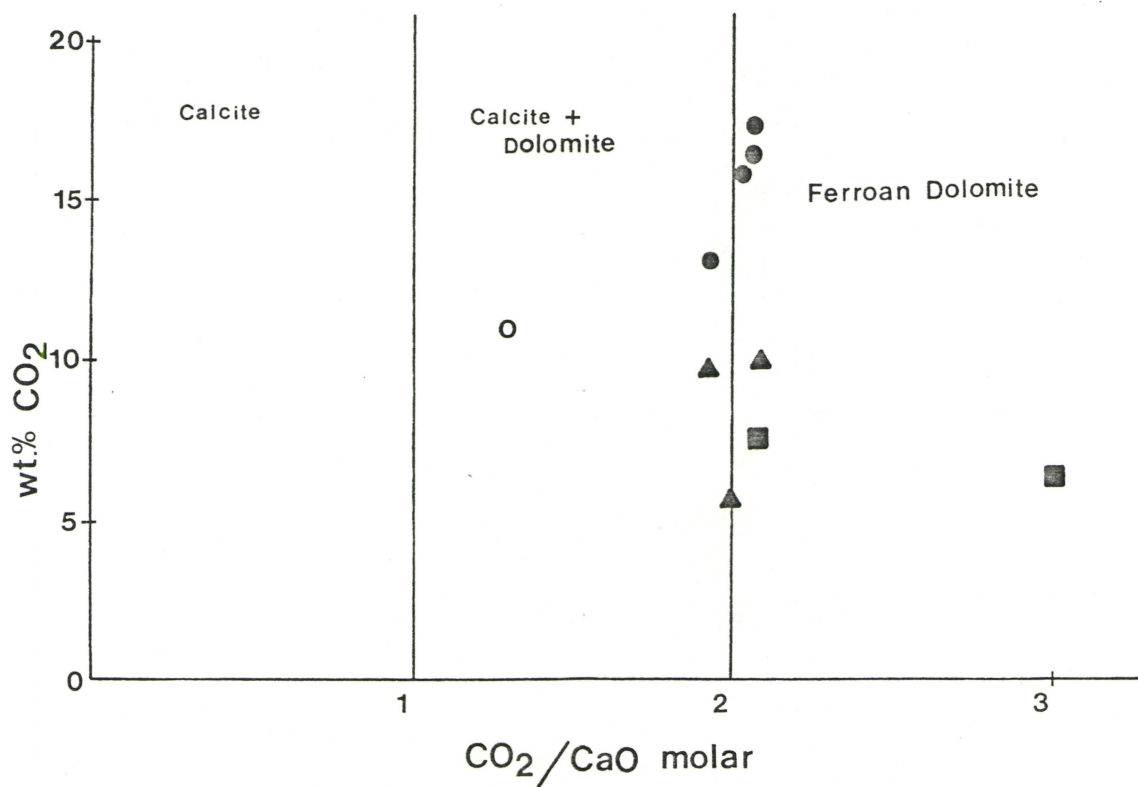
written by F.Block and G.Mattison, Penn State University). Normative calcite, magnesite, and siderite are included in the mineral norm calculation. Where normative calcite and magnesite have similar abundances dolomite is the normative carbonate present. The normative siderite value is a reflection of carbonate solid solution with iron. The normative siderite value may also be affected by the presence of iron in silicates, oxides, and sulphide which were not included in the magnetite and ilmenite values. Calcite is probably present in samples which have normative calcite values in excess of magnesite normative values.

Sample RX68000 has a normative calcite value greater than twice its normative magnesite. These values suggest that calcite is present along with dolomite in the sample. Some of the auriferous syenites and gneissic syenite samples such as RX67980 and RX67993 have normative calcite and magnesite which suggest that some calcite is present. Samples RX68000 and RX67980 were shown to have calcite present by XRD analysis. Thus, there appears to be a correlation between the presence of calcite and high gold levels.

The CO<sub>2</sub> content in a given sample generally reflects the amount of carbonate present. It does not measure the intensity of carbonate alteration. The process of carbonitization is dependent on the availability of Ca, Mg and Fe in the rock. Temperature and CO<sub>2</sub> fugacity are also controls involved with carbonitization (Davies et al, 1982).

Figure 8 is a plot of  $\text{CO}_2$  versus  $\text{CO}_2/\text{CaO}$  molar ratio. This diagram shows the fields of carbonate minerals based on molar ratios of the cation oxide ( $\text{CaO}$ ) and  $\text{CO}_2$ . At  $\text{CO}_2/\text{CaO}$  molar ratios of  $<1$  calcite should be the only carbonate present. Ratios between 1 and 2 show that calcite and dolomite or ankerite are both present. With  $\text{CO}_2/\text{CaO}$  molar ratios of greater than 2 only dolomite or ankerite are present. Davies et al (1982) compared the mineralogy as a function of  $\text{CO}_2/\text{CaO}$  ratio (as in Fig.8) with carbonate types determined from XRD on a set of samples from the Timmins area. They found that in most cases the  $\text{CO}_2/\text{CaO}$  molar ratios correctly identified the carbonate type.

At McBean most samples cluster around the  $\text{CO}_2/\text{CaO}$  ratio of 2. The auriferous syenitic rocks appear to have some calcite with the majority of the carbonate in the form of ferroan dolomite. As the degree of alteration increases and  $\text{CO}_2$  fugacity increases the formation of dolomite is favoured over calcite. This is shown at McBean by highly altered rocks such as the talc-chlorite schist and mafic syenite which plot in the ferroan dolomite field. The presence of some calcite in the highly auriferous samples suggests that these rocks were subjected to at least two phases of carbonitization. A second less intense phase of carbonitization is probably responsible for the calcite formation. The fluids which caused the formation of calcite may also have carried the gold in solution.



<100 ppb ●  
 >10 ppm ○  
 100-1000 ppb ■  
 >10 ppb ▲

FIGURE 8 Theoretical Fields of Carbonates on a Plot of CO<sub>2</sub> versus CO<sub>2</sub>/CaO molar ratio

## 5.2 Trace Element Geochemistry

An analysis of 26 elements for 10 samples across the level 1 ore zone was carried out Nuclear Activation Services using instrumental neutron activation. The results of these analyses are presented in Table 3. An interelement correlation coefficient matrix was calculated to determine trends among the various elements. The formula for  $r$  can be found in Appendix 3. The correlation coefficients were tested for significance using the Student's  $t$  distribution. The formula for calculating Student's  $t$  can also be found in Appendix 3. Correlation coefficients which are significant at the 1% level and coefficients which are probably significant at the 5% are shown in Table 4.

At McBean there is a significant positive correlation between Au and Sm, Ce, La, W and U. The correlations between Au and Ce, W, and U are significant at the 1% level (this means there is a 1 in 100 chance that the correlation is due to chance). The correlations between Au and Sm, Lu are probably significant at the 5% probability level. There is therefore a positive correlation between some of the rare earth elements and gold. In addition there are also positive correlations between the light and heavy rare earth elements. These correlations will be discussed elsewhere in this study.

The McBean ore body has distinctive trace element associations which differ from the typical Archean lode gold deposit and from other deposits in the Larder Lake-Kirkland



Table 3. Trace Element Abundances by INAA

Element	Units	RX67973	RX67974	RX67980	RX67993	RX67996
Ag	ppm	<5	<5	<5	<5	<5
As	ppm	3	<2	<2	4	<3
Au	ppb	250	900	1200	1200	770
Ba	ppm	400	200	900	1300	300
Ca	%	4	2	2	4	4
Co	ppm	14	10	12	28	29
Cr	ppm	230	220	100	280	200
Fe	%	2.77	2.51	3.90	3.97	6.11
Hf	ppm	2	2	2	1	2
Mo	ppm	<5	<5	6	8	<5
Na	%	4.1	5.0	6.1	3.1	4.5
Ni	ppm	<200	<200	<200	<200	<200
Sb	ppm	0.7	0.4	0.3	0.9	1.6
Sc	ppm	9.7	6.7	4.3	8.6	16.6
Se	ppm	6	<5	<5	<5	<5
Ta	ppm	<1	<1	<1	<1	<1
Th	ppm	4.1	3.6	4.2	3.5	4.2
U	ppm	<1.0	1.0	1.9	1.9	1.7
W	ppm	6	17	8	17	14
Zn	ppm	<50	<50	<50	<50	70
La	ppm	21	22	31	25	28
Ce	ppm	34	37	54	46	61
Sm	ppm	3.5	3.6	5.2	4.8	6.6
Eu	ppm	0.7	1.0	1.1	1.2	1.6
Yb	ppm	0.9	0.9	1.1	1.2	1.7
Lu	ppm	0.21	0.19	0.24	0.21	0.29

Table 3. cont'd

Element	Units	RX68000	RX67897	RX67986	RX67990	RX67997
Ag	ppm	<5	<5	<5	<5	<5
As	ppm	4	27	<3	<2	<3
Au	ppb	15000	23	14	7	<10
Ba	ppm	200	2200	400	6700	300
Ca	%	5	2	4	6	5
Co	ppm	41	12	31	22	28
Cr	ppm	140	130	140	260	180
Fe	%	9.14	2.20	7.30	4.88	6.01
Hf	ppm	<1	3	2	1	2
Mo	ppm	<5	<5	<5	<5	15
Na	%	2.8	7.0	3.6	2.4	4.4
Ni	ppm	<200	<200	<200	<200	300
Sb	ppm	1.2	1.3	1.4	1.0	1.2
Sc	ppm	15.3	3.3	23.0	19.2	17.4
Se	ppm	<8	<5	<5	<5	<7
Ta	ppm	<1	<1	<1	<1	<1
Th	ppm	3.2	2.5	3.1	1.4	4.5
U	ppm	4.9	2.4	2.2	<1.2	1.9
W	ppm	65	<5	<5	<7	<8
Zn	ppm	80	<50	110	90	100
La	ppm	45	32	22	16	32
Ce	ppm	98	51	40	27	61
Sm	ppm	9.7	6.2	5.8	3.8	6.8
Eu	ppm	2.0	2.2	1.5	0.7	2.0
Yb	ppm	1.9	0.4	1.7	0.8	1.8
Lu	ppm	0.30	0.05	0.26	0.19	0.26

Table 4 Interelement Correlation Coefficient Matrix

	As	Au	Ba	Ca	Co	Cr	Fe	Hf	Mo	Na	Sb
Lu	<b>-.81</b>				.67		.76				
Yb					<b>.84</b>		<b>.88</b>				
Eu											
Sm		.75			.73		.76				
Ce		<b>.83</b>									
La		.76									
Zn				.67			.74				
W		<b>.98</b>									
U		<b>.89</b>			.67		.70				
Th			<b>-.84</b>								
Sc				.79	.71		.76			<b>-.70</b>	
Sb											
Na				<b>-.86</b>	<b>-.68</b>			<b>.88</b>			
Mo											
Hf				<b>-.68</b>							
Fe		.64*			<b>.92</b>						
Cr											
Co				.69							
Ca											
Ba											
Au											

	Sc	Th	U	W	Zn	La	Ce	Sm	Eu	Yb
Lu										<b>.90</b>
Yb										
Eu						.76		<b>.83</b>		
Sm			<b>.91</b>	.71		<b>.90</b>	<b>.94</b>			
Ce			<b>.89</b>	<b>.82</b>		<b>.96</b>				
La			<b>.87</b>							
Zn	<b>.92</b>									
W			<b>.84</b>							
U										
Th										

-**bold** type = correlation coefficient is significant at the 1% level

-plain type = correlation coefficient is probably significant at the 5% level

\* = correlation coefficient just below probable significance at the 5% level

Lake area. Abundant, mobile base metal elements such as Cu, Zn, Pb and Co are usually concentrated 1 to 5 times background levels in gold deposits (Kerrich, 1981). At McBean Zn and Co are not enriched from background levels in Archean syenites. For comparison to McBean the trace element abundances from felsic syenites at the Macassa Mine are listed below.

Unaltered Felsic Syenite\*

Au(17ppb) Ag(-) As(3.5) Sb(3.1) Sc(8.1) Cr(80) Co(24) Ni(18)  
Zn(56) W(3) U(3.2) Th(26) Ba (817)

\*average of 3 rocks

Altered and Mineralized Felsic Syenite

Au(900ppb) Ag(<1) As(6.0) Sb(5) Sc(5) Cr(70) Co(0) Ni(17)  
Zn(98) W(41) U(3.1) Th(21) Ba(531)

-units in ppm except as noted

-analysis from Kerrich and Watson, 1984.

W, As, Sb, Hg and B are often highly concentrated in gold bearing rocks. Arsenic is commonly present in the form of arsenopyrite in gold deposits. Arsenic concentrations are typically 1000 to 10,000 ppm in lode gold deposits (Kerrich, 1981). The association of arsenic with gold mineralization in the Timmins area has been documented by Fyon and Crockett (1981) and Davies et al (1982). At McBean only weak, sporadic enrichments of arsenic occur. These small enrichments do not correlate with gold abundances and no arsenopyrite mineralization was observed at the mine.

Cr and W are immobile elements which can be significantly enriched in gold deposits. Cr is found in



elevated abundances at McBean compared with Cr levels in syenites at Macassa. Though Cr levels are elevated at McBean there is no correlation between Cr and Au in the ore zone at level 1. Tungsten is commonly found as scheelite and can occur in gold bearing veins and in chemical sediments (Kerrick, 1981). High concentrations of tungsten are commonly characteristic of deep seated deposits (Boyle, 1979). Tungsten concentrations in syenitic rocks at McBean display a very close correlation with gold. The tungsten concentration reaches 65 ppm in sample RX68000 where the Au value is 15 ppm. The tungsten concentration is less than 8 ppm in non-auriferous rocks.

Uranium concentrations exhibit a good correlation with gold concentrations at McBean. Uranium is found in elevated concentrations in various types of skarns, veins and lodes. Its use as an indicator element is largely confined to specific mineral belts (Boyle, 1979). Thorium/uranium ratios average from 3 to 4:1 in igneous rocks (Arhens, 1965). In sample RX68000 which contains 15 ppm of gold the Th/U ratio is 0.65:1. In igneous rocks uranium and thorium are usually concentrated in accessory minerals such as: monazite, sphene, apatite and alanite. In sample RX67973 apatite was observed using the SEM. In this sample the Th/U ratio is greater than 4:1. At McBean elevated U concentrations may not be due to increases in the amount of accessory minerals, but, in the proportion of uranium in these minerals. It is more likely that the elevated uranium level are related to

carbonitization. The uranyl ion  $(UO_2)^{2+}$  may be the cause of the elevated concentrations of U as it can form soluble carbonate complexes.

The % of Fe in the McBean samples versus Au has a correlation coefficient of 0.64 . This r value is below the 5 % level of probable significance, but, does indicate some positive correlation between Fe and Au. This relationship is due to a pyrite-gold association as noted in the ore petrography.

Enrichments of As (1 to 5X), Sb (5 to 50X) and W (2 to 100X) occur in syenites with anomalous Au concentrations at Macassa. These elevated As, Sb and W abundances are thought to reflect the postcrystallization penetration of hydrothermal fluids into the syenites along microfractures. This process is thought to occur coevally with gold mineralization (Kerrick and Watson, 1984). A similar process probably occurred at McBean. Numerous carbonate and quartz veinlets with carbonate linings can be found in the altered syenitic rocks. These veinlets probably formed along fractures emplaced by intense localized folding and shearing associated with the Larder Lake Break.

In summary, the trace element data shows that As and Sb are not present in concentrations significantly above background while W and U are significantly enriched in auriferous syenitic rocks.

### 5.3 Rare Earth Element Geochemistry

As stated previously, a significant correlation exists between some of the rare earth elements (REE) and gold. The REE are useful in that they provide a signature in rocks which can give clues to their magmatic origin and alteration history. Partial melting and fractional crystallization effect the original REE abundances in rocks. The absolute concentrations of REE can be controlled by the fractional crystallization of small amounts of minerals such as sphene, allanite, hornblende and apatite (Henderson, 1984). REE abundances from one rock type to another are best compared by normalization to chondrite meteorite values; this is the rock REE abundance is divided by the chondrite meteorite REE abundance. The chondrite normalization values used in this study are Masuda values divided by 1.2. They are as follows:

La	0.315
Ce	0.813
Sm	0.192
Eu	0.0722
Yb	0.208
Lu	0.0323

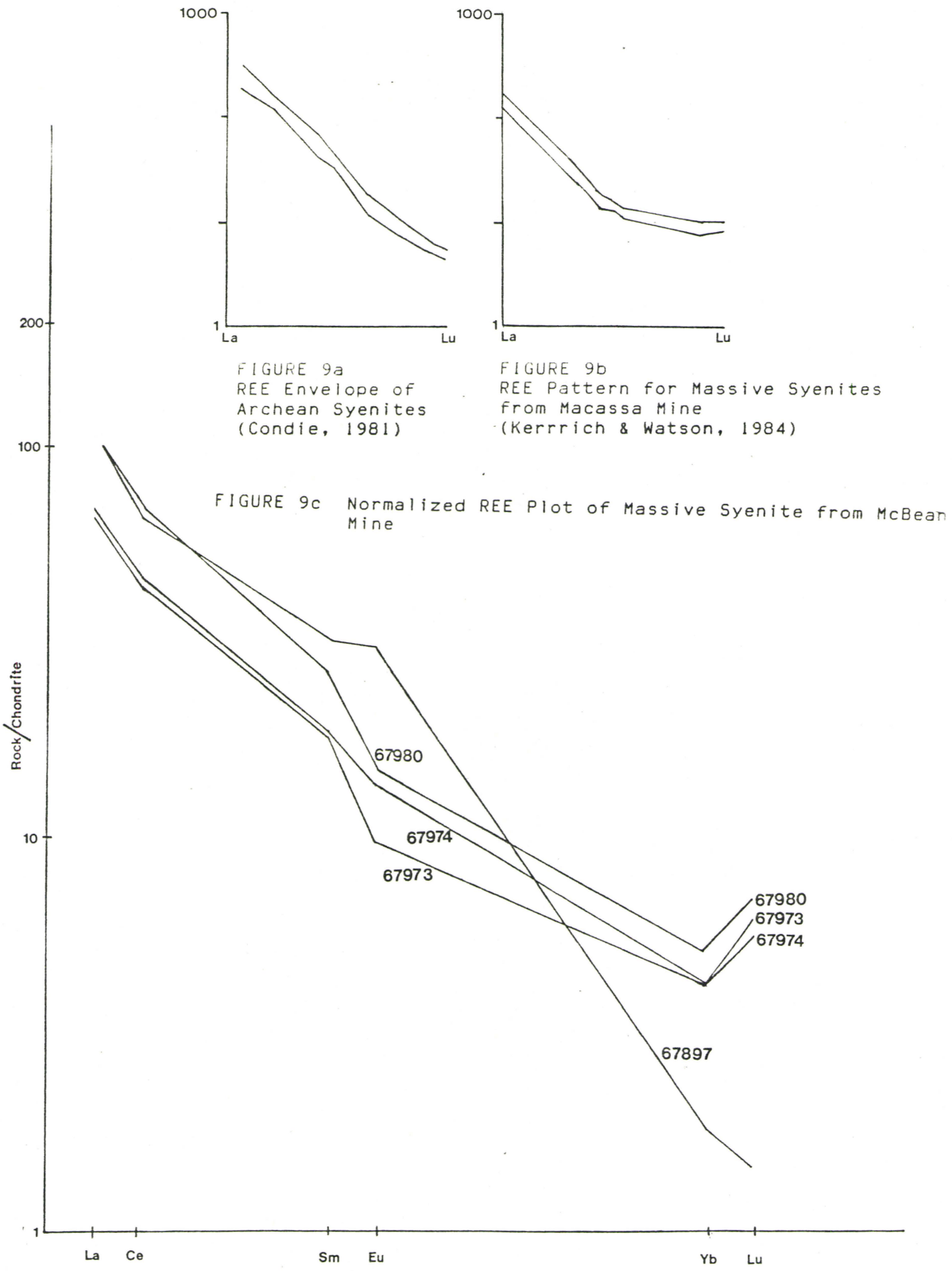
(Jahn and Sun, 1979).

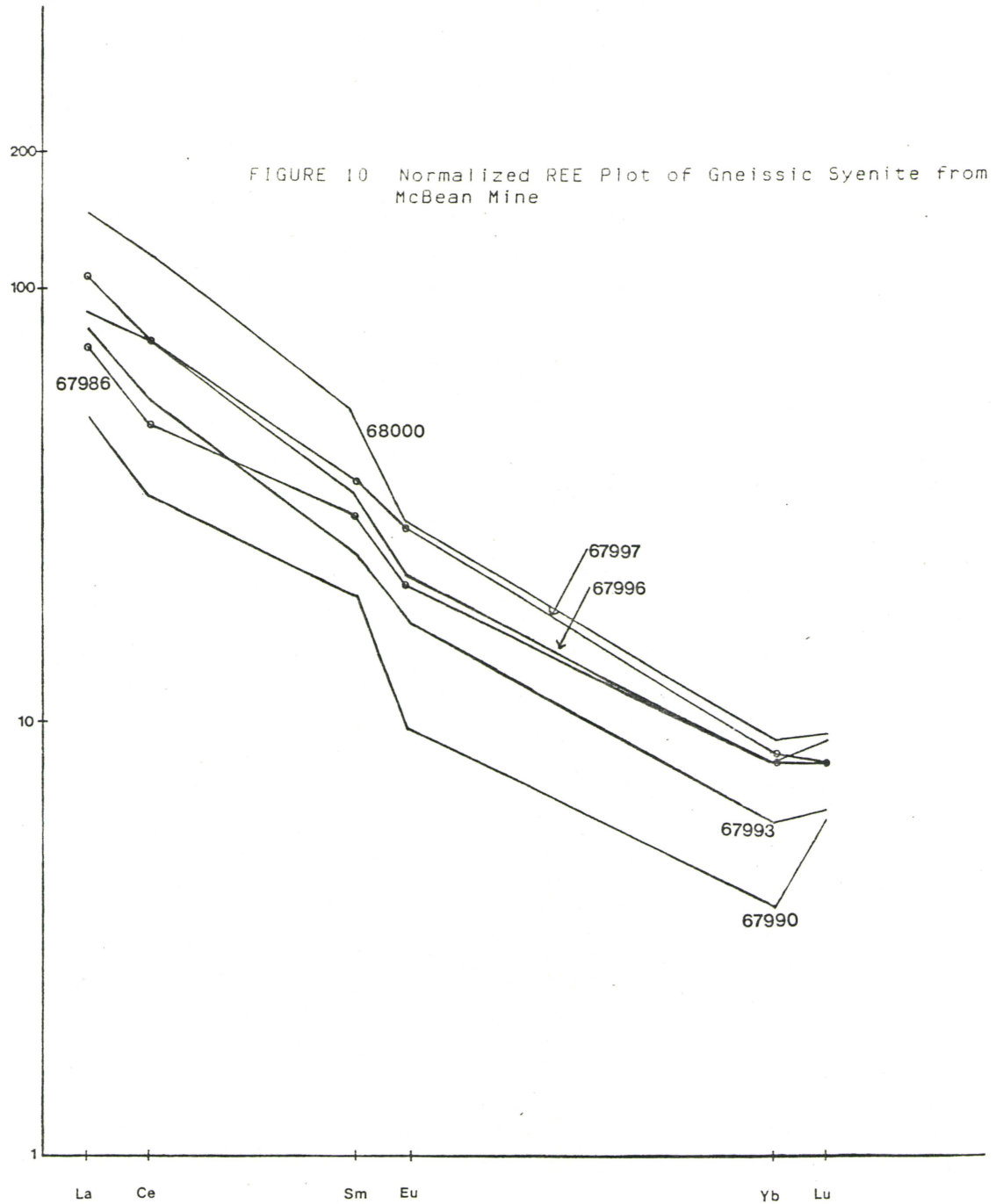
When rock/chondrite values are plotted against atomic number an anomaly in the Eu value is often present. Primary Eu anomalies are commonly attributed to the ease in which Eu can be reduced from  $\text{Eu}^{3+}$  to  $\text{Eu}^{2+}$  and removed from magma by the separation of plagioclase feldspar (Bowden et al, 1979). Negative Eu anomalies can be produced when sediments with abundant feldspar such as a metagraywacke undergo partial

melting (Cullers and Graf, 1984). Jensen (1985) believes that syenite intrusives in the Timiskaming were produced by the partial melting of sediments. This may be the cause of primary negative Eu anomalies in the syenitic rocks at McBean.

The high amount of carbonate in the various rock types at McBean suggest that the carbonate is of hydrothermal origin.  $\text{CO}_2$  vapour tends to concentrate REE and especially light REE (LREE)(Cullers and Graf, 1984). As seen in a comparison of the typical Archean syenite REE envelope (Fig.9a) with the normalized plots of syenitic rocks from McBean (Figures 9c and 10) no LREE enrichment due to carbonitization is present. As with the Macassa Mine massive syenite REE envelope (Fig.9b) there is a slight heavy REE (HREE) enrichment at McBean over the typical Archean syenite REE envelope. During hydrothermal alteration REE can be complexed as carbonate, fluoride and sulphate complexes in alkaline solutions. It is believed this complexing plays a dominant role in the transport of REE (Herman, 1972 in Kerrich and Fryer, 1978). With increasing atomic number these complexes become more stable. This results in the enrichment of the heaviest REE in latest stage deposits as these stable complexes are the last to break down (Kerrich and Fryer, 1978). These complexes may break down and precipitate REE due to a decrease in pressure, fixation of  $\text{CO}_3^{-2}$  or a change in alkalinity. This may account for the







HREE enrichment above the norm in Archean syenites at the McBean and Macassa mines.

As seen in Figures 9c and 10 the syenites and gneissic syenites show La is 50 to 150 times the chondrite value at McBean while the HREE are 4 to 10 times the chondrite values. The samples all display negative Eu anomalies. The true drop in the Eu value below the slope of the plot cannot be seen as no Gd analyses were performed. Other rocks in the Kirkland Lake area such as lamprophyre dikes at the Canadian Arrow Deposit near Matheson contain no Eu anomaly. These dikes are interpreted as mantle derivatives injected along transcrustal fractures (McNeil and Kerrich, 1985). Some of the altered massive syenites at the Macassa Mine show a moderate negative Eu anomaly. In the augite syenite at Macassa a K-feldspar, actinolite, quartz, chlorite fracture system displays a pronounced negative Eu anomaly compared with nearby unaltered augite syenite. This negative Eu anomaly is thought to result from the hydrolysis of plagioclase (Kerrich and Watson, 1984). Quartz veins and banded hydrothermal quartz veins at the Dome Mine have very low normalized REE abundances (between 1 and 40 times chondrite values). These veins also exhibit a strong positive Eu anomaly. The low abundance of REE is thought to be a direct relation to the amount of hydrothermal quartz present. The carbonate probably carries the REE and the hydrothermal quartz acts as a dilutant (Kerrich and Fryer, 1979). This same dilutant effect with quartz appears to occur at McBean also (see

Figures 11 and 12). Kerrich and Fryer believe that the positive Eu anomaly at Dome is consistent with the reduced state of solution involved in the emplacement of the deposit which is suggested by the predominance of  $Fe^{2+}$ . The anomalous normalized abundance of Eu is very dependent on the redox potential of the rock/water system. Kerrich and Fryer (1979) believe this Eu anomaly at Dome provides independent evidence for chemical exchange between the rocks and solutions of low redox potential.

Sample RX67897 is from a syenite unit south of the level 1 ore zone at McBean. The chondrite normalized REE pattern of this rock is compared with three syenite samples from the ore zone (see Fig.8c). Sample RX67697 displays a highly fractionated REE typical of Archean syenites, but, it has lower REE abundances. Sample RX67897 is only weakly carbonitized, coarse grained and contains 3% coarse grained euhedral pyrite. The three samples from the ore zone syenites are more highly carbonitized, contain carbonate veinlets, and have 10% fine grained (<1.5mm) pyrite. Compared with sample RX67897 the syenites from the ore zone are enriched in HREE and display a much greater Eu anomaly. Sample RX67897 shows the original REE distribution of the syenite before alteration. The syenite REE patterns from the ore zone are an example of hydrothermal overprinting of the original REE distribution. Bowden et al (1979) found similar REE patterns in hydrothermally altered syenites and granites in the Ririwai lode deposit in Nigeria. They found the



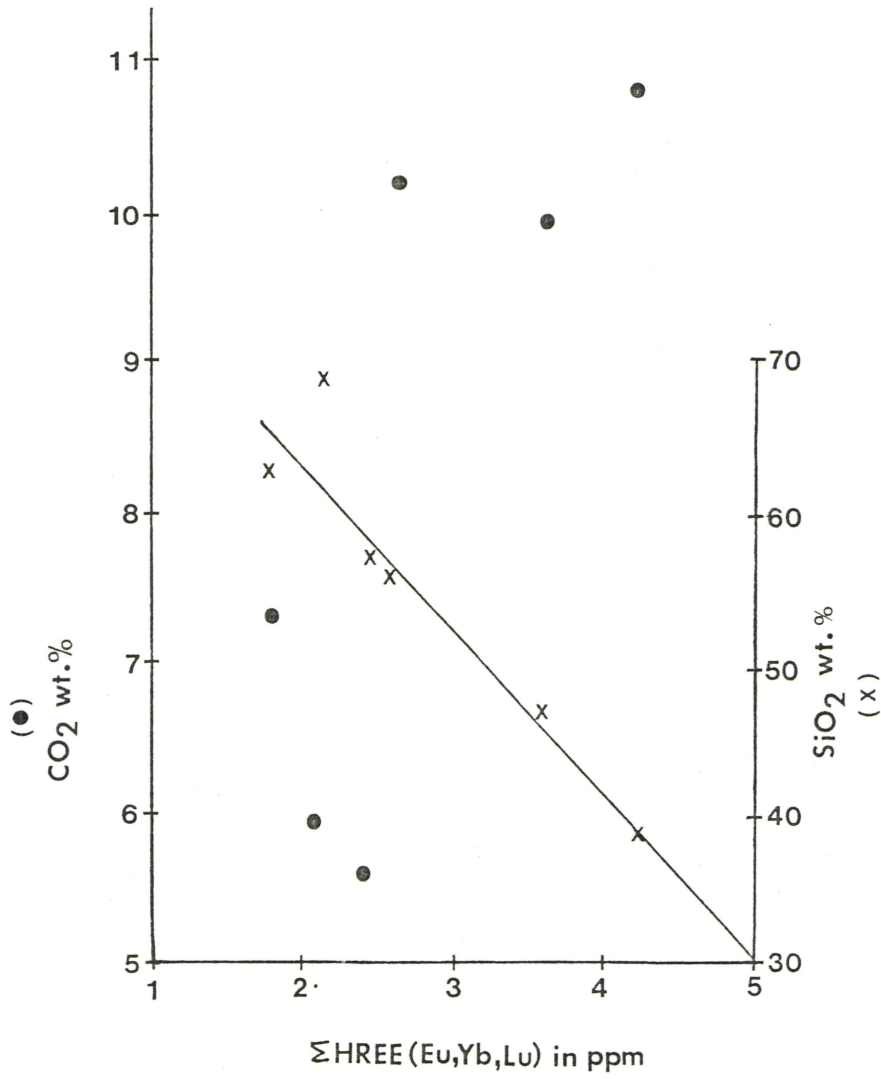


FIGURE 11 Plot of  $\Sigma\text{HREE}$  versus  $\text{SiO}_2$  and  $\text{CO}_2$

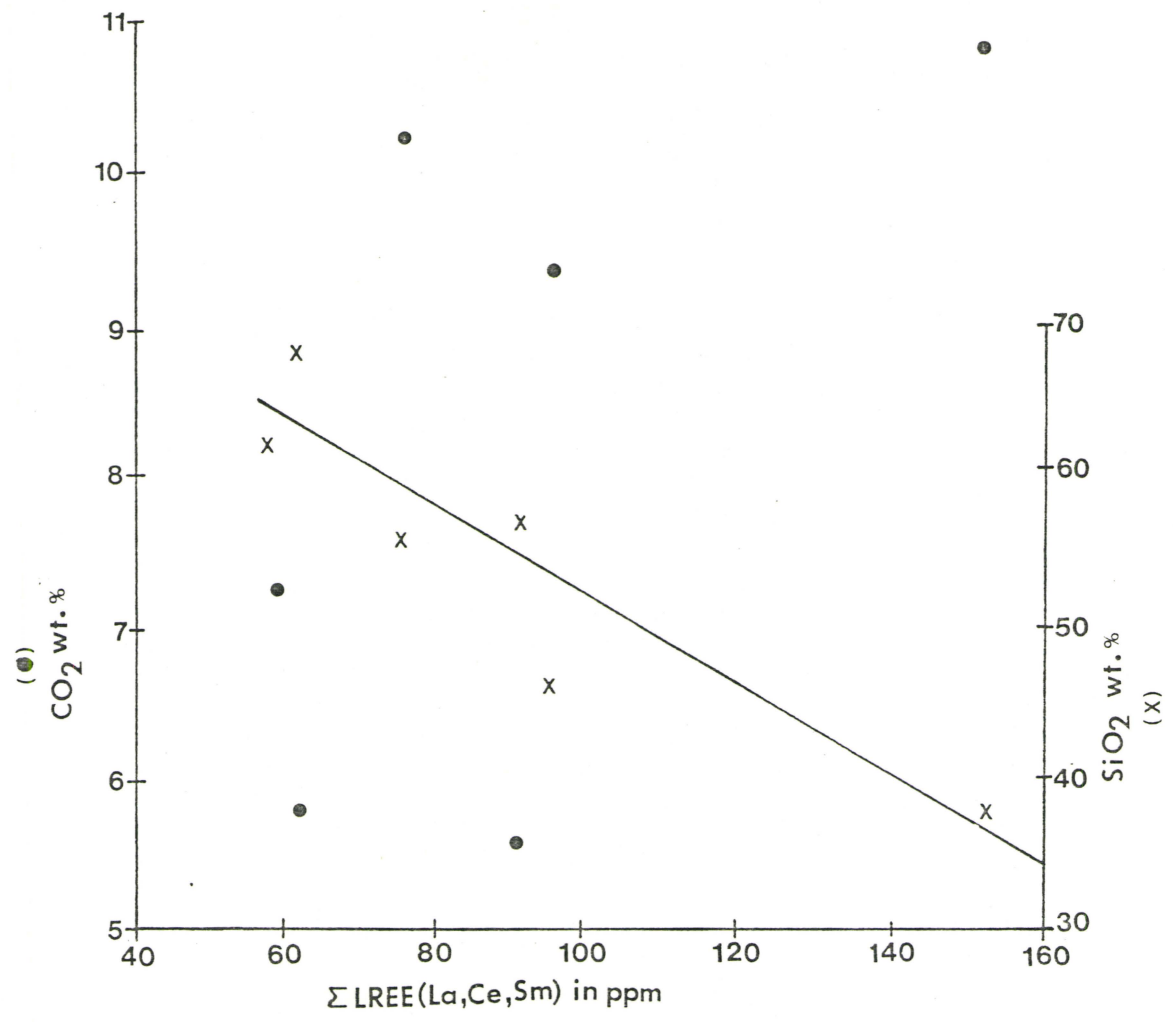


FIGURE 12 Plot of  $\Sigma$ LREE versus SiO<sub>2</sub> and CO<sub>2</sub>

altered zone to have elevated REE abundances and the magnitude of the negative Eu anomaly to be increased.

At McBean the elevated HREE distribution is probably due to the late stage precipitation of carbonate complexed with HREE. Hydrothermal carbonitization has depleted the ore zone Eu abundances relative to less altered syenite. In the ore zone gold concentrations vary in proportion with REE abundances. The higher gold values are found in the samples with the greater REE abundances (see Fig.9c). In gneissic syenites north of the ore zone a pronounced negative Eu anomaly is also present as are elevated HREE concentrations compared with the Archean syenite envelope and sample RX67897.

The gneissic syenites north of the ore zone show poor Au-REE abundance correlations. The 15 ppm Au sample (RX68000) has elevated REE abundances, but, the other samples north of the ore zone display little correlation between Au and REE concentrations. The REE patterns north of the ore zone are similar. It is the LREE and HREE abundances which vary. This variation is probably due to a quartz dilution effect. Plots of  $\text{SiO}_2$  wt.% versus HREE and LREE concentrations confirm this (see Figures 11 and 12). The  $\text{CO}_2$  wt.% may positively correlate with REE concentrations. When plotted the relationship between the two is not clear except that samples with high LREE and HREE concentrations tend to contain a high  $\text{CO}_2$  wt.%. Thus, at the McBean Mine the auriferous syenites are enriched in HREE, they display a

greater negative Eu anomaly compared to less altered syenites, and there is a correlation between REE concentrations and Au in the ore zone.



## CHAPTER 6 CONCLUSIONS, RECOMMENDATIONS FOR FURTHER RESEARCH AND EXPLORATION IN THE LARDER LAKE AREA

### 6.1 Conclusions

The gold mineralization at McBean is doubtlessly due to its proximity to the Larder Lake Break. The fault system associated with the Break may have initiated as fracturing and slumping along the margins of early calc-alkaline volcanic piles caused by the weight of accumulating ultramafic lava (Jensen, 1981). The syenitic intrusions probably formed from the partial melting of sediment adjacent to calc-alkaline volcanics. These intrusions were preferentially emplaced in the zone of deformation associated with the Larder Lake Break. Further deformation along the Break fractured and folded the syenitic intrusives.

The Larder Lake Break served as a major conduit for rising hydrothermal fluids. These fluids were responsible for the extensive carbonitization at McBean. Alteration at McBean is also characterized by ubiquitous pyrite and locally abundant chlorite. As carbonate alteration was extensive, the hydrothermal solutions involved were probably alkaline in nature.

The gold emplaced at McBean may have been mobilized from carbonaceous sediments by metamorphic and hydrothermal waters. These waters were probably driven upward by magmatic heat. Gold may have carried in these solutions as compounds with carbonate and bisulphide. The presence of magnetite may

have triggered gold precipitation. Gold values are generally associated with high concentrations of fine grained pyrite. Gold was observed as free grains in gangue and as inclusions and platings with pyrite. Auriferous syenitic rocks at McBean have elevated tungsten and uranium abundances. Arsenic and antimony are commonly found in elevated abundances in other deposits of the Larder Lake-Kirkland Lake gold camp. These elements are found in only background levels at McBean. The auriferous syenitic rocks contain elevated HREE abundances and greater negative Eu anomalies compared with typical Archean syenites.

The gold at McBean may have precipitated from solutions associated with a particular phase of carbonatization. SEM results show carbonate composition to vary with the type of carbonate (example: vein or non-vein carbonate). XRD results point to the fact that auriferous syenitic rocks contain some minor calcite along with dolomite, while talc-chlorite schist wall rocks contain only dolomite. This may be the result of calcite being associated with fracture filling of the more competent units.

Thus, the gold mineralization at McBean is a result of the interplay of several factors. Sediments flanking an older volcanic pile concentrated gold. Rising hydrothermal and metamorphic water took gold into solution from these rocks. The Larder Lake Break acted as a major fluid conduit along which gold bearing solutions rose. The syenitic

intrusives at McBean then acted as a preferential site for gold precipitation to occur.

## 6.2 Recommendations for Further Research and Exploration in the Larder Lake Area

Microprobe analysis of carbonates from deposits associated with the Kirkland Lake-Larder Lake Break would establish if gold mineralization in hydrothermally altered rocks is related with a particular type of carbonate. At McBean, isotopic studies would reveal the temperature and origin of mineralizing hydrothermal fluids.

Future gold exploration in the Larder Lake area should include examination of felsic intrusive bodies in proximity to the Larder Lake Break and associated zones of deformation. Particular attention should be paid to zones of carbonate alteration. Samples should be stained in the field to determine the presence of iron bearing carbonate. Zones of pyritization, chloritization and silicification should also be examined closely. In geochemical surveys W,U and REE should be analysed for in addition to Au, As and Sb.

## REFERENCES

- AHRENS, L.H. 1965. Distribution of the Elements in our Planet. McGraw-Hill Book Company. 110p.
- BOWDEN, P., BENNETT, J.N., WHITLEY, J.E., and MOYERS, A.B. 1979. Rare Earths in Nigerian Mesozoic Granites and Related Rocks, in Ahrens, L.H. (Ed.), Origin and Distribution of the Elements. Pergamon Press, pp. 479-492.
- BOYLE, R.W. 1979. The geochemistry of gold and its deposits: Canada Geol. Survey, v. 28, 584p.
- COLVINE, A.C., ANDREWS, A.J., CHERRY, , MACDONALD, J.A., SPRINGER, J., FYON, J.A., LAVIGNE, M., MARMONT, S., and DUROCHER, M.E. 1984. An intergrated model for the origin of Archean lode gold deposits: Ontario Geological Survey, Open File Report 5524, pp. 1-98.
- CONDIE, K.C. 1981. Archean greenstone belts: Developments in Precambrian geology, v. 3, 434p.
- CULLERS, R.L., and GRAF, J.L. 1984. Rare Earth Elements in Igneous Rocks of the Continental Crust: Intermediate and Silicic Rocks-Ore Petrogenesis, in Henderson, P. (Ed.), Rare Earth Element Geochemistry. Elsevier, 315p.
- DAVIES, J.F., WHITEHEAD, R.A., CAMERON, R.A., and DUFF, D. 1982. Regional and Local Patterns of CO<sub>2</sub>-K-Rb-As Alteration: A Guide to Gold in the Timmins area, in Geology of Canadian Gold Deposits, CIM Special v. 24, pp. 130-143.
- DOWNES, M.J. 1981. Structural and Stratigraphic Aspects of Gold Mineralization in the Larder Lake Area, Ontario, in Genesis of Archean, Volcanic-Hosted Gold Deposits, Symposium held at the University of Waterloo, March 7, 1980, Ontario Geological Survey, MP 97, pp. 66-69.
- FYON, J.A., and CROCKET, J.H. 1981. Volcanic Environment of Carbonate Alteration and Stratiform Gold Mineralization, Timmins area, in Genesis of Archean, Volcanic-Hosted Gold Deposits, Symposium held at the University of Waterloo, March 7, 1980, Ontario Geological Survey, MP 97, pp. 47-57.
- FYON, J.A., CROCKET, J.M., and SCHWARCZ, H.P. 1983. Magnesite abundance as a guide to gold mineralization associated with ultramafic flows, Timmins area: J. Geochem. Explor., 18: 245-266.



- GILLES, J.E., and BANCROFT, M.G. 1985. An XPS and SEM study of gold deposition at low temperatures on sulphide mineral surfaces: concentration of gold by adsorption/reduction: *Geochimica et Cosmochimica Acta*, v. 49, pp. 979-987.
- HENDERSON, P. 1982. Inorganic Geochemistry. Pergamon Press, 353p.
1984. General Geochemical Properties and Abundances of the Rare Earth Elements, in Henderson, P. (Ed), Rare Earth Element Geochemistry. Elsevier, pp. 1-29.
- HEWITT, D.F. 1963. The Timiskaming series of the Kirkland Lake area: *Can. Mineral.*, v. 7, pp. 479-522.
- JAHN, B.M., and SUN, S.S. 1979. Trace Element Distribution and Isotopic Composition of Archean Greenstones, in Ahrens, L.H. (Ed.), Origin and Distribution of the Elements. Pergamon Press, pp. 587-596.
- JENSEN, L.S. 1981. Gold Mineralization in the Kirkland Lake-Larder Lake Area, in Genesis of Archean, Volcanic-Hosted Gold Deposits, Symposium held at the University of Waterloo, March 7, 1980, Ontario Geological Survey, MP 97, pp. 59-65.
- JENSEN, L.S., and LANGFORD, F.F. 1985. Geology and Petrogenesis of the Archean Abitibi Belt in the Kirkland Lake Area, Ontario; Ontario Geological Survey, Miscellaneous Paper 123, 130p.
- JOLLY, W.T. 1978. Metamorphic History of the Archean Abitibi Belt, in Metamorphism in the Canadian Shield, Geological Survey of Canada, Paper 78-10, pp. 63-78.
- KERRICH, R. 1981. Archean Gold-Bearing Sedimentary Rocks and Veins: A Synthesis of Stable Isotope and Geochemical Relations, in Genesis of Archean, Volcanic-Hosted Gold Deposits, Symposium held at the University of Waterloo, March 7, 1980, Ontario Geological Survey, MP 97, pp. 144-167.
- KERRICH, R., and FRYER, B.J. 1979. Archaean precious-metal hydrothermal systems, Dome Mine, Abitibi greenstone belt II. REE and oxygen isotope relations: *Can. J. Earth Sci.*, v. 16, pp. 440-458.
- KERRICH, R. and WATSON, G.P. 1984. The Macassa Mine Archean gold deposit, Kirkland Lake, Ontario: geology, patterns of alteration, and hydrothermal regimes: *Econ. Geol.*, v. 79, pp. 1104-1130.

- LOVELL, H., GRABOWSKI, G., GUINDON, D., and BATH, A. 1986. Kirkland Lake Resident Geologist Area, Northern Region, in Report of Activities 1985, Regional and Resident Geologists, edited by C.R. Kustra, Ontario Geological Survey, Miscellaneous Paper 128, pp. 179-225.
- MCINNES, B.I. 1985. Ore petrography and wallrock alteration studies at the Lake Shore Mine, Kirkland Lake, Ontario. Unpublished B.Sc. thesis, McMaster University.
- MCNEIL, A.M., and KERRICH, R. 1986. Archean lamprophyre dykes and gold mineralization, Matheson, Ontario: the conjunction of LILE-enriched mafic magmas, deep crustal structures, and Au concentration: *Can. J. Earth Sci.*, v. 23, pp. 324-343.
- NORCLIFFE, G.B. 1982. Inferential Statistics for Geographers. Hutchinson & Co. Ltd. 263p.
- PHILLIPS, G.N., GROVES, D.I., and MARTYN, J.E. 1984. An epigenetic origin for Archean banded iron-formation-hosted gold deposits: *Econ. Geol.*, v. 79, pp. 162-171.
- RIDLER, R.H. 1970. Relationship of mineralization to volcanic stratigraphy in the Kirkland-Larder Lake Area, Ontario: *Geol. Ass. Can. Proc.*, v. 21, pp. 33-48.
- STEWART, P. 1986. The association of gold to simple shear deformation in greenstone trachytes. Unpublished B.Sc. thesis, University of Waterloo.
- THOMSON, J.E. 1943. Geology of Gauthier Township, East Kirkland Lake area. 50th Annual Report, v. L, Part viii, Ontario Dept. of Mines.
1943. Geology of McGarry and McVittie Townships, Larder Lake area. 50th Annual Report, vol. L, Part vii, Ontario Dept. of Mines.
1950. Geology of Teck Township and the Kenogami Lake area. Ontario Dept. of Mines, Annual Report of 1948, v. 57, Part v, pp. 1-53.
- TIHOR, L.A., and CROCKET, J.H. 1976. Origin and distribution of gold-bearing carbonate zones of the Kirkland Lake-Larder Lake area, Ontario: *Geol. Surv. Can.*, Paper 76-1A, pp. 407-408.
- TIHOR, S.L. 1978. The mineralogical composition of the carbonate rocks of the Kirkland Lake-Larder Lake gold camp. Unpublished M.Sc. thesis, McMaster University.

- TOOGOOD, D.D, and HODGSON, C.J. 1985. A structural investigation between the Kirkland and Larder Lakes Gold Camps; Ontario Geological Survey, Miscellaneous Paper 119, pp. 200-204.
- TULLY, D.W. 1963. The geology of the Upper Canada Mine: Geol. Ass. Can. Proc., v. 15, pp. 61-86.
- WHITEHEAD, R.E.S., DAVIES, J.F., CAMERON, R.A., and DUFF, D. 1981. Grant 30 Carbonate, alkali and arsenic anomalies associated with gold mineralization, Timmins area, in Ontario Geological Survey Miscellaneous Paper 98, pp. 318-333.

APPENDIX I CONDENSED SAMPLE DESCRIPTIONS AND GOLD ASSAYS

- RX67897: Syenite, massive, fine grained, to 5% py  
(10 ppb)
- RX67898: same as RX67897  
(<5 ppb)
- RX67899: Talc-Chlorite Schist, foliation at 058/90  
(<5 ppb)
- RX67900: same as RX67899  
(15 ppb)
- RX67969: Mafic Syenite, massive, medium grained (to 3mm),  
to 15% py  
(<5 ppb)
- RX67970: same as RX67969  
(<5 ppb)
- RX67971: Gneissic Syenite, well banded, fine grained,  
(<5ppb) banding at 031/72E, mixture of coarse and fine  
grained py to 15%, py more pervasive along  
fractures
- RX67972: Sheared Mafic Syenite  
(<5 ppb)
- RX67973: Syenite, massive, fine grained, reddish, mixture  
(320 ppb) of coarse and fine py to 15%
- RX67974: same as RX67974  
(900 ppb)
- RX67975: Gneissic Syenite, coarse grained, biotite rich  
(45 ppb) layers barren of py, felsic layers mixture of  
coarse and fine py
- RX67976: Mafic Syenite, medium grained (to 3mm)  
(<5 ppb)
- RX67977: Mafic Syenite, fine grained  
(<5 ppb)
- RX67978: Syennite lens, fine grained, 12cm wide at base  
(<5 ppb)
- RX67979: same as RX67977  
(10 ppb)
- RX67980: Syenite, fine grained to 20% py  
(1.21 ppm)



APPENDIX 1 cont'd

- RX67981: Dioritic Gneiss, weak banding, coarse grained  
(50 ppb)
- RX67982: same as RX67981 with finer grain size  
(55 ppb)
- RX67983: same as RX67981 with finer grain size  
(<5 ppb)
- RX67983: Mafic Syenite, massive, fine grained  
(20 ppb)
- RX67985: Gneissic Syenite, weak banding, fine grained, to  
(10 ppb) 10% py
- RX67986: Gneissic Syenite, weak banding, fine-med. grained  
(5 ppb) 10% py, highly magnetic
- RX67987: Micaceous Mafic Syenite  
(<5 ppb)
- RX67988: Syenite, fine-med. grained, 10% py  
(<5 ppb)
- RX67989: Micaceous Mafic Syenite, gneissic banding, highly  
(<5 ppb) foliated
- RX67990: Syenite, fine-med. grained, numerous qtz veinlets,  
(<5 ppb) magnetic, 10% py
- RX67991: Talc Schist-Mafic Syenite  
(<5 ppb)
- RX67992: Gneissic Syenite, weakly banded, biotite present  
(5 ppb)
- RX67993: Qtz vein with Syenitic material, width 12cm,  
(2.11 ppm) orientation 100/75S, 15% py
- RX67994: Talc-Chlorite Schist  
(10 ppb)
- RX67995: Gneissic Syenite, fine grained, well banded  
(15 ppb) banding at 094/90
- RX67996: Gneissic Syenite, well banded, coarse and fine py  
(1.02 ppm) to 5%
- RX67997: Gneissic Syenite, well banded, magnetic, fine  
(15 ppb) grained py to 5%

APPENDIX 1 cont'd

- RX67998: Talc-Chlorite Schist  
( $<5$  ppb)
- RX67999: Gneissic Syenite, well banded, magnetic, coarse py  
( $<5$  ppb) to 15%
- RX68000: Gneissic Syenite, well banded, magnetic, 25% py  
(15.8 ppm)
- RX84501: Feldspar Porphyry, massive, fine grained  
(25 ppb)
- RX84502: same as RX84501  
( $<5$  ppb)
- RX84503: Massive Syenite from Level 5  
(5 ppb)
- RX84504: Massive Syenite from Level 5, magnetic, purplish  
(5 ppb) colour

APPENDIX 2 SEM X-Ray Emissions

<u>Analysis Location</u>	<u>Element</u>	<u>Energy</u>	<u>Counts</u>	<u>Mineral</u>
RX67980				
1	Na	1.05	2472	Albite
	Al	1.49	16890	
	Si	1.74	71379	
2	Mg	1.26	7150	Carbonate
	Ca	3.69	72241	
	Ca	4.01	8711	
	Mn	5.89	1041	
	Fe	6.40	7429	
	Fe	7.06	867	
3	Ti	4.51	2604	Ilmenite
	Fe	6.40	112399	
	Fe	7.05	14611	
RX67971				
1	Mg	1.26	2281	Carbonate
	Ca	3.69	23335	
	Ca	4.01	2855	
	Fe	6.39	2650	
2	Al	1.49	3536	K-spar
	Si	1.74	12554	
	K	3.31	1107	

APPENDIX 2 cont'd

<u>Analysis Location</u>	<u>Element</u>	<u>Energy</u>	<u>Counts</u>	<u>Mineral</u>
RX67973,Ci				
1	Si	1.74	152211	Quartz
2	Mg	1.26	6012	Carbonate
	Ca	3.69	74792	
	Ca	4.02	9082	
	Mn	5.90	624	
	Fe	6.40	7902	
	Fe	7.05	995	
3	Na	1.04	2395	Plagioclase
	Al	1.49	15479	
	Si	1.74	72107	
	K	3.31	9376	
4	S	2.30	160622	Pyrite
	Fe	6.40	66931	
	Fe	7.06	8646	
RX67973,Cii				
1	Mg	1.26	10214	Carbonate
	Ca	3.69	76998	
	Ca	4.01	9511	
	Mn	5.89	771	
	Fe	6.40	8756	
	Fe	7.06	1111	



APPENDIX 2 cont'd

<u>Analysis Location</u>	<u>Element</u>	<u>Energy</u>	<u>Counts</u>	<u>Mineral</u>
RX67973,Cii				
2	Al	1.49	16107	K-spar
	Si	1.74	71621	
	K	3.31	39597	
	K	3.60	4096	
RX67899				
1	Mg	1.26	13249	Carbonate
	Ca	3.69	83578	
	Ca	4.01	9743	
	Mn	5.89	869	
	Fe	6.40	5329	
	Fe	7.05	711	
2	Mg	1.26	7572	Carbonate
	Ca	3.69	78437	
	Ca	4.01	9571	
	Mn	5.90	937	
	Fe	6.40	5858	
	Fe	7.04	697	

APPENDIX cont'd

<u>Analysis Location</u>	<u>Element</u>	<u>Energy</u>	<u>Counts</u>	<u>Mineral</u>
RX67899				
3	Mg	1.26	9770	Carbonate
	Ca	3.69	80739	
	Ca	4.01	9593	
	Mn	5.89	916	
	Fe	6.40	5360	
	Fe	7.05	773	
4	Mg	1.26	11872	Carbonate
	Ca	3.69	84715	
	Ca	4.02	9895	
	Mn	5.88	665	
	Fe	6.40	5507	
	Fe	7.06	712	

APPENDIX 3 Calculation of Correlation Coefficient ( $r$ )  
and Student's  $t$

Let  $X$  be the dichotomous variable, and each observation on  $X$  will be scored either 0 or 1.

$N_0$  is the number of individuals classed with 0 on  $X$ .

$N_1$  is the number of individuals classed with 1 on  $X$ .

Hence  $N = N_0 + N_1 =$  the total number of observations.

$Y$  is a continuous variable that is divided into two sub-groups by  $X$ . The means of these two sub-groups are denoted by  $\bar{Y}_0$  and  $\bar{Y}_1$  respectively where

$$\bar{Y}_0 = \frac{\sum Y_{0i}}{N_0}$$

$$\bar{Y}_1 = \frac{\sum Y_{1i}}{N_1}$$

The standard deviation of  $Y$  ( $\hat{s}_Y$ ) is

$$\hat{s}_Y = \sqrt{\frac{N \sum Y^2 - (\sum Y)^2}{N(N-1)}}$$

When these quantities have been calculated, then  $r$  can be obtained from

$$r = \frac{\bar{Y}_1 - \bar{Y}_0}{\hat{s}_Y} \sqrt{\frac{N_1 N_0}{N(N-1)}}$$

As in the case of Spearman's  $r_s$ , this correlation coefficient is tested for significance against Student's  $t$  distribution with  $N - 2$  degrees of freedom. In this case,

$$t = r \sqrt{\frac{N-2}{1-r^2}}$$